Trackable metallodrugs combining luminescent Re(I) and bioactive Au(I) fragments

Andrés Luengo,[†] Vanesa Fernández-Moreira, [†]* Isabel Marzo[‡] and M. Concepción Gimeno[†]*

[†]Departamento de Química Inorgánica, Instituto de Síntesis Química y Catálisis Homogénea (ISQCH), CSIC-Universidad de Zaragoza Pedro Cerbuna 12, 50009, Zaragoza, Spain

[‡]Departamento de Bioquímica y Biología Molecular, Universidad de Zaragoza, Pedro Cerbuna 12, 50009, Zaragoza, Spain.

KEYWORDS. Rhenium, Gold, Anticancer, Theranostic, Luminescence, Microscopy

Abstract: Heterobi- and tri-metallic complexes have been synthesized by the combination of different metallic fragments, a luminescent Re(I) species and a bioactive Au(I) derivative. A ditopic P,N-donor ligand (L) was used as linker between both metals, affording six new complexes of the type *fac*-$[Re(bipy)(CO)_3(LAuCl)]^+$ (**4**-**6**) and $[(fac\text{-}[Re(bipy)(CO)_3(L)])_2Au]^{3+}$ (**7**-**9**) after a thorough synthetic procedure. Their emission is associated with a ^{3}MLCT (Re(dπ)→bipy(π*)) transition and red shifted in polar solvents with lifetimes in the range of ns and quantum yields values up to 12.5 %. Cytotoxicity values in A549 cells of heterotrimetallic species are almost twice than for the heterobimetallic (c.a. 37 *vs* 69 μM respectively), being the L-Au fragment the source of the antiproliferative activity. Species **7**

and **8** showed similar behaviour by fluorescence microscopy, with a non-uniform cytoplasmatic distribution, a clear accumulation in single spots at the edge of the inner cell membrane as well as in areas within the nucleus. Preliminary studies suggest the DNA as one of the targets and passive diffusion the entrance pathway.

Introduction

The design of trackable anticancer drugs has become a priority in our society since it provides the possibility of understanding how drugs actually interact with the biomolecules in the body.[1] Such crucial information would surely deliver great advances in the development of new therapeutics that could efficiently reach a larger number of diseases. Among the metal-based therapeutic agents, gold complexes stand as one of the most studied so far. Their antiarthritic properties have been used in medicine since the early 80s.[2] At the moment, two of these gold drugs, auranofin and aurothiomalate, are at the stage of clinical trials for the treatment of certain cancers.[3] Mechanistically, the mitochondria, thioredoxin reductase, and pathways of oxidative phosphorylation are believed to be among the primary intracellular targets.[4] However, the perfect understanding of their chemical behavior is still unclear.[5] A reasonable approach to tackle this problem could be the development of gold based trackable drugs. Incorporation of a luminophore into the structure of a gold complex would enable the visualization of the probe by fluorescence microscopy. Such technique could provide information regarding their internalization mechanism, biodistribution, localization, biological targets and their interaction. Using organic fluorophores as optical probes are the most common method to develop trackable gold-based therapeutic agents. Acridine, anthracene, naphthalimide, coumarine and BODIPY among others have been recently used to visualize the cellular biodistribition of gold complexes, Figure 1.[6] Despite their good commercial availability and relatively simple chemistry to be incorporated to gold complexes,

their photophysical properties are not ideal for bioimaging purposes. Apart from the particular case of BODIPY, whose emission is determined by the substituents,[7] their fluorescence in the UV region, short lifetimes and high lipophilicity are some of the characteristics that need to be improved to provide optical probes that can be used for in vivo applications, where tissue light penetration is a handicap.[8]

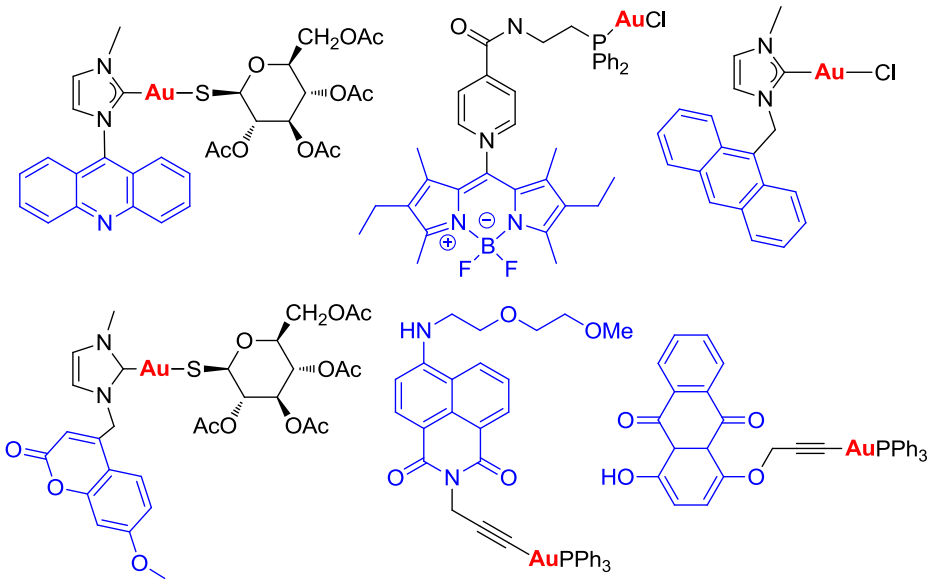

Figure 1. Gold based probes based on the incorporation of a luminophore.

Alternatively, some luminescent metal complexes, such as Ru(II)[9] and Re(I)[10] species have been also combined with gold(I) complexes to afford bimetallic trackable species (Figure 2). The phosphorescence nature of their emission makes these probes suitable candidates to be used as cell imaging agents.[11] However, building the bimetallic compounds is not always easy, and a thoughtful synthetic strategy needs to be followed considering the different stability and compatibility of the metal complexes and ligands. Thus, if the two complexes have enough stability, they could be first synthesized separately and then coupled together.[10] In this way, tedious purification steps could be

avoided. A second strategy would be the design of bifunctional chelating ligands that are able to selectively bind each metal center. This strategy is particularly complicated when similar metals are used.[12] An alternative synthetic approach would be a stepwise pathway, with the synthesis of the first metal complex, the posterior insertion of the ancillary chelating ligand following by coordination of the second metal atom.[13] Therefore, it is not surprising that, the synthetic pathway for delivering trackable probes bearing two metals could be extremely complicated and it should be carefully planned. Despite the synthetic complexity that may involve the design of trackable gold species bearing luminescent metal complexes as luminophores, we are determined to deepen into this field. At the moment, the vast majority of investigations deal with the use of organic chromophores as optical probes, therefore, our work was directed towards the design of heterometallic Re(I)/Au(I) and Re(I)/Au(I)/Re(I) complexes. A thorough study of their photophysical properties as well as the analysis of their cytotoxicity in human A549 lung cancer cell line was made. Furthermore, their application as cell imaging agents was also investigated.

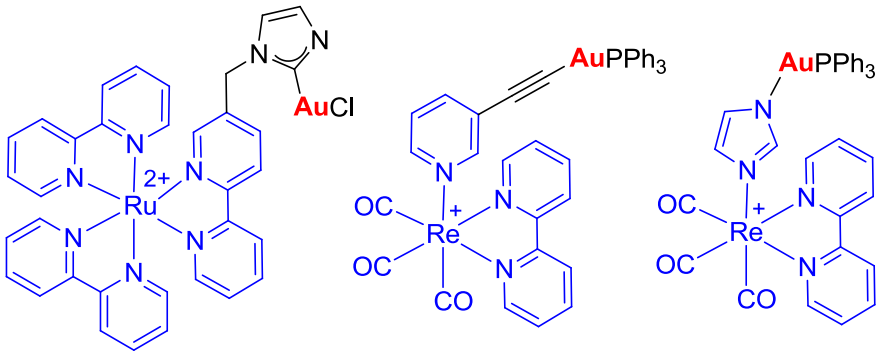

Figure 2. Bimetallic gold probes.[9,10]

Results and Discussion

Synthetic approach

In a previous study we have demonstrated that it is possible to visualize gold(I) complexes in cancer cells by combination with a luminescent Re(I) fragment and using an alkyne as linker.[10] In the present work the focus is set on the development of heterometallic Re(I)/Au(I) complexes where a phosphine derivative is the linker between the two metal centers. However, working with phosphine derivatives is not always straightforward due to their easy oxidation. Thus, a thorough synthetic pathway needs to be established. The first approach taken was the preparation of ditopic ligands (**L1** and **L2,** Scheme 1), followed by two subsequent coordination steps. The key aspect is to build ligands that are able to selectively bind each metal center. Since gold(I) complexes have a great affinity to be coordinated to phosphines and Re(I) to pyridine derivatives, N-(diphenylphosphino)ethylamidepyridine derivatives were synthesized. The synthesis was performed via Schotten-Baumann reaction between either isonicotinoyl chloride or a nicotinoyl chloride derivative with 2-(diphenylphosphino)ethylamine affording **L1** and **L2** respectively.[14] Thereafter, coordination reaction of ligands **L1** and **L2** with [AuCl(tht)] (tht = tetrahydrothiophene) was performed. As expected, the metal was selectively bonded to the phosphorus donor atom affording complexes **1** and **2**, leaving the nitrogen available for further coordination, see Scheme 1 (Synthetic approach A). Despite the rigorous handling of the reagents, trying to avoid the oxidation of the phosphine, a percentage of the oxidized product was always present. Therefore, a different synthetic route was considered. The 2-(diphenylphosphino)ethylamine (**L0**) would be first protected from oxidation by coordination to the metal centre generating species **3**, and then the synthesis of the amide species **1** and **2** would take place, see Scheme 1 (Synthetic approach B). This new procedure resulted in overall better yields and purity of the final products.

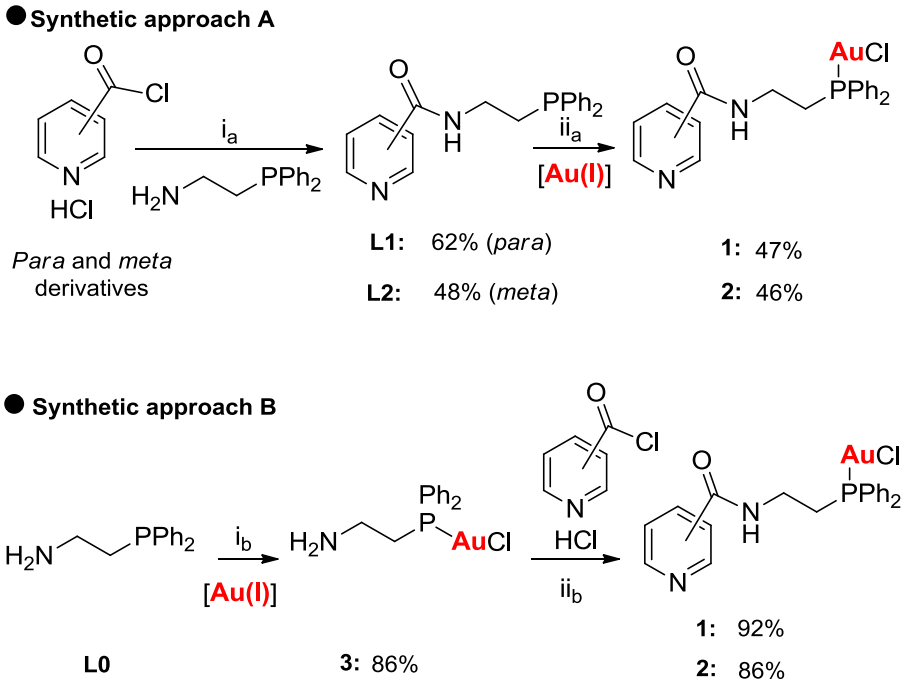

Scheme 1. Synthetic approach A: (i_a) 2-(diphenylphosphino)ethylamine, Et_3N, dichlorometane, rt, 12 h, under Ar. (ii_a) [AuCl(tht)], dichloromethane, 1 h, rt., under Ar. Synthetic approach B: (i_b) [AuCl(tht)], dichloromethane, 1.5 h, rt., under Ar. (ii_b) acylchloride derivative, Et_3N, dichlorometane, rt, 12 h.

Following the synthetic approach B, the percentage of oxidized phosphine was diminished to a minimum and a lone peak in the $^{31}P\{^1H\}$ spectrum was observed at 24.8, 24.8 and 28.7 ppm for compounds **1**, **2** and **3** respectively, Table S1. Those values are in concordance with $^{31}P\{^1H\}$ NMR chemical shifts displayed by similar complexes.[15]

The next step of the synthetic procedure was the coordination of the second metal center. As previously commented, Re(I) derivatives were selected as the luminescent probes. Specifically, *fac*-[Re(bipy)$(CO)_3(CF_3SO_3)$] (**A**) was used as the reactive Re(I) complex, where the substitution of the

triflate ligand by pyridine derivatives have been widely described.[15] However, the product of the reaction of **A** with either **1**, **2** or **3** did not afford a single product. Instead, a mixture of heterobimetallic **4**-**6** and heterotrimetallic **7**-**9** complexes was obtained, see Scheme 2. The different heterobi- and tri-metallic species have been isolated and purified by column chromatography. A plausible explanation for the unanticipated mixture could be related with the easiness with which rhenium activated species are able to capture a chloride ion.

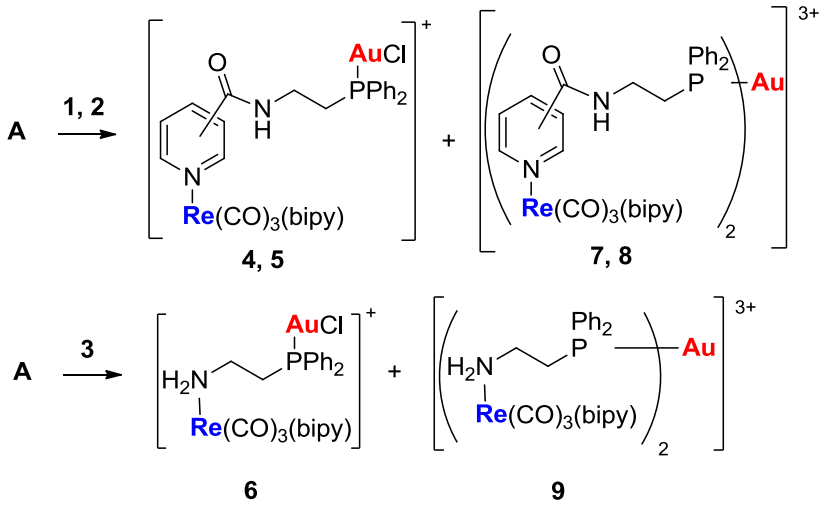

Scheme 2. Synthesis of the heterometallic Re-Au complexes. **L1**, **1**, **4** and **7** correspond to the *para* derivatives and **L2**, **2**, **5** and **8** to the *meta* derivative. Compounds **6** and **9** were obtained from complex **3**.

A previous work described by Coogan and coworkers[17] describes the synthetic difficulties to obtain a rhenium complex bearing a chloropyridine derivative as ligand. The problem was mainly due to the presence of chloride ions in the reaction media that were reverting the activated rhenium complex, $[Re(bipy)(CH_3CN)(CO)_3]OTf$ to the precursor complex, $[Re(bipy)Cl(CO)_3]$ (**B**) (Scheme 3).[17] The same idea could be perfectly applied in the present case. Thus, the activated rhenium complex **A** in

presence of **1**, **2** and **3** could lead to the formation of the expected heterobimetallic complexes **4**, **5** and **6** respectively, together with the precursor rhenium complex **B** and highly reactive gold species **C** bearing a labile triflate ligand, see Scheme 3. Thereafter, the instability of **C** would prompt its reaction with **4**, **5** and **6** and with unreacted precursor **A** (Scheme 3, synthetic route A) or alternatively, **C** could also decompose to afford a more stable bis(phosphine) gold species, that thereafter would react with two equivalents of **A** (Scheme 3, synthetic route B). This theory has been confirmed by two different facts: First, extraction of **B** as one of the side products from the column chromatography performed for the purification of all the complexes and secondly, by the yield improvement of complex **4**-**9** upon the addition of a second equivalent of **A**.

Alternatively, a different synthetic route was considered to be able to exclusively synthesise the heterotrimetallic species. Thus, compounds **7**, **8** and **9** were prepared after the synthesis of the correspondent gold bis(phosphine) derivatives **10** and **11**, see Scheme 3. Such procedure entailed the use of the stable gold(I) complex $[Au(tmbn)_2]OTf$, where tmbn is 2,4,6-trimethoxybenzonitrile, for the *in situ* preparation of cationic bis(phosphine) gold(I) species bearing the 2-(diphenylphosphino)ethylamine ligand, that can further react with the isonicotinoyl chloride or a nicotinoyl chloride derivative to give complexes **10** and **11** respectively. Then, the bis(phosphine) complexes were allowed to react with **A** affording **7**, **8** and **9** in reasonable yields, 50, 18 and 47%. Infrared spectra for the heterobi- and tri-metallic species **4**-**9** showed two strong carbonyl stretching bands, ν(CO), between 1894 and 2027 cm^{-1} corroborating the cationic character of these species as well as the approximate C3v symmetry and consequently, the facial configuration of the carbonyl ligands.[18] Moreover, $^{31}P\{^1H\}$ NMR spectroscopy studies confirmed the proposed gold coordination mode in all cases, either the P-Au-Cl (c.a. 22 ppm) or the P-Au-P (c.a. 34 ppm), see Table 1. Further ^1H, $^{13}C\{^1H\}$

NMR, UV-vis spectroscopy and analytical data provided by mass spectrometry corroborated the accomplishment on the synthesis of all complexes**.**

Table 1. Carbonyl IR stretching bands and $^{31}P\{^{1}H\}$ NMR chemical shifts (CD_2Cl_2) of **4**–**9**.

	IR(ν(CO))	$^{31}P\{^{1}H\}$(ppm)		IR(ν(CO))	$^{31}P\{^{1}H\}$(ppm)
4	2028, 1905	22.6	**7**	2027, 1902	34.5
5	2029, 1904	20.8	**8**	2027, 1902	34.5
6	2021, 1894	23.6	**9**	2021, 1894	34.9

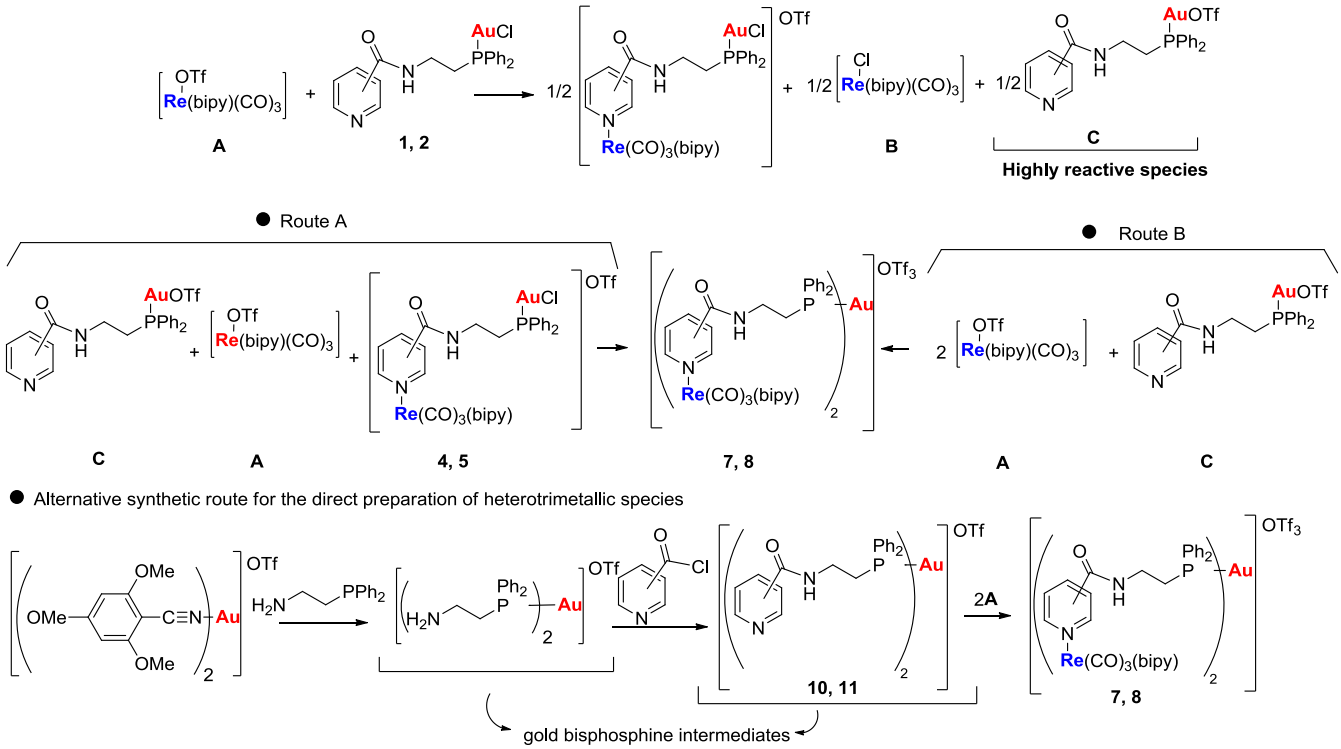

Scheme 3. Proposed mechanism for the formation of complex **7** and **8** from the reactive gold species **C**. Synthesis of complexes **6** and **9** would follow the same scheme. Alternative synthetic route for the direct preparation of heterotrimetallic species.

Photophysical properties

UV-visible absorption spectra were recorded for complexes **4**-**9** in a degassed DCM solution at 298 K. All of them showed an absorption profile that can be defined as a combination of the typical absorption pattern of bisimine Re(I) derivatives with that of gold(I)diphenylphosphene fragment , i.e. ligand centered transitions (^{1}LC) at higher energies (≤ 320nm) and a metal-to-ligand-charge-transfer transition (^{1}MLCT) at lower energies (c.a. 375 nm).[19] Specifically, ^{1}LC transitions can be attributed to $\pi\rightarrow\pi^*$ transitions among bipyridine, pyridine and phenyl units, and the ^{1}MLCT transitions are assigned basically to Re(dπ)→L(π^*) transitions, being those of the bipyridine the main contributor, Figure S1. Moreover, it is noteworthy that heterotrimetallic species have about twice the value of molar extinction coefficient than the heterobimetallic complexes for the ^{1}MLCT transition and even higher values are seen for the ^{1}LC band. Such variation agrees with intercomponent electronic energy transfer in heteropolinuclear complexes that normally associates the absorption and emission spectra based on additive properties of the different metallic fragments.[20] The most significant absorption data are collected in Table 2.

Table 2. UV-vis absorption bands and extinction coefficients for complexes **4**-**9**. (Degassed CH_2Cl_2 solution at 298 K ($2.5E^{-5}$ M)).

Species	**λ_{abs} / nm, (ε / dm^3 mol^{-1} cm^{-1})**
4	235 (26100), 273 (17400), 320 (10600), 368 (3800)
5	237 (27300), 272 (16200), 320 (8300), 364 (3400)
6	236 (28700), 279 (13400), 321 (9000), 326 (3600)
7	240 (52200), 273 (36600), 319 (22000), 371 (6700)

8	239 (61300), 267 (41600), 320 (20400), 360 (7200)
9	238 (43900), 280 (24800), 321 (16300), 362 (6300)

Further emissive properties of complexes **4**-**9** were analyzed in degassed DCM and DMSO solution at 298 K (Figures 3 and S2 and Table 3). All of them showed a broad emission spectrum, whose maximum is red shifted upon changing the solvent from DCM to DMSO. The observed red shift could be attributed to a further stabilization of the excited states in polar solvent, which is in agreement with the emission pattern seen for similar complexes reported in the literature.[21] Specifically, the behavior of the complexes could be divided into two groups, those containing a pyridine derivative in their coordination sphere (**4**, **5**, **7** and **8**) and those presenting a 2-(diphenylphosphino)ethylamine (**6** and **9**).

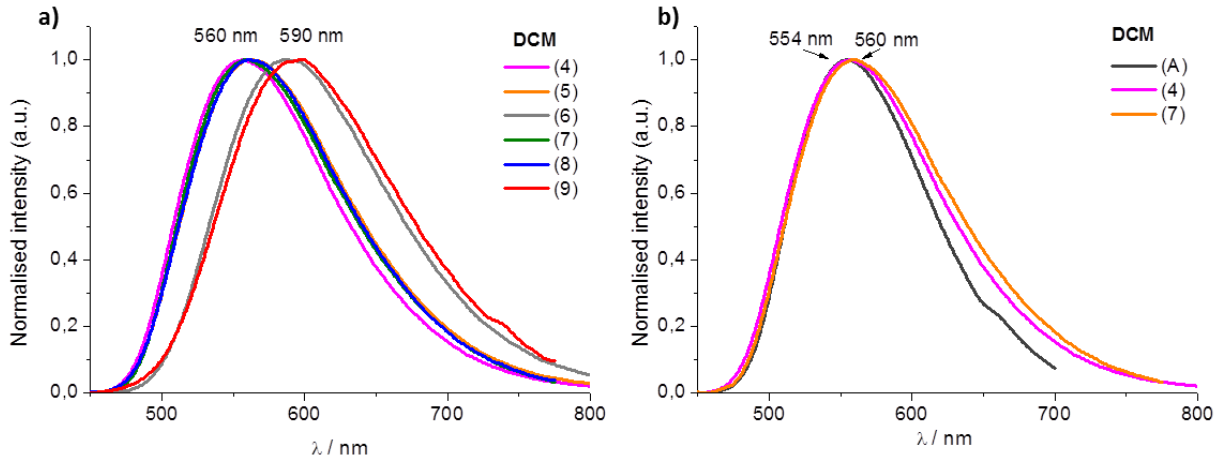

Figure 3. (a) Normalized emission spectra of complexes **4**-**9** in CH_2Cl_2 solution and (b) normalized emission spectra of complexes **4**, **7** and **A** (fac-[Re(bipy)$(CO)_3(CF_3SO_3)$]) in CH_2Cl_2 solution.

The formers showed emission maxima around 560 nm in DCM that shift to c.a. 585 nm in DMSO, whereas the second group showed their emission maxima at c.a. 590 nm in DCM that is also red shifted in DMSO to c.a. 608 nm. In all cases the emission could be attributed to ^{3}MLCT transition, a Re(dπ)→bipy(π*) transition,[22] where the gold atom does not seem to affect the luminescence properties. The excited state lifetimes were measured in both solvents solution, corroborating the phosphorescence nature of the emissions. Thus, complexes **4**, **5**, **7** and **8** presented lifetime values over 200 ns in DCM solution. Instead, complexes **6** and **9** barely reached 110 ns. As before, when the solvent was changed from DCM to DMSO, an expected higher stabilization of the MLCT excited state would take place prompting easier non-radiatively processes which would lead to lower lifetime values.[23,21b] The differences seen on the emission and lifetime values between the species containing either pyridine or amine derivatives could be attributed to the different electronic effect exerted into the HOMO orbitals. Since (diphenylphosphino)ethylamine is believed to have a greater electron donor character than the pyridine derivatives, complexes **6** and **9** would have their homo orbitals destabilized in comparison with those of complexes **4**, **5**, **7** and **8** producing red shifted emission values and shorter lifetimes. Quantum yield values varied from 3 to 12.5 %, which are considerably higher than those reported for monometallic rhenium complexes (table 3).[24] Thus, the combination of Re(I) and Au(I) within a single molecule seems to be an extraordinary approach to design high valuable luminophores. Additional luminescence studies were performed in order to assess the stability of the complexes in biological media. Specifically, complex **4** and **9** were dissolved in DMSO and then added to a PBS solution (pH 7.4, final DMSO concentration ≤ 0.5%), the emission spectra were registered at t = 0, 0.3 and 18 hours. No loss of luminescence was observed suggesting that no disruption of the complexes had taken place (Figure S3). The same behavior was observed by ^{1}H-NMR experiments performed during 2 days for the same complexes in a DMSO-d6 solution.

Table 3. Excitation, emission lifetimes and quantum yields of complexes **4**-**9**.

Species	**λ_{exc} (nm)**	**λ_{em} (nm)**	**ζ (ns)**	**φ**
4	427[a]	556[a]	269[a]	12.5[a]
	406[b]	582[b]	119[b]	-
5	427[a]	560[a]	304[a]	9.2[a]
	406[b]	584[b]	112[b]	-
6	435 [a]	587 [a]	107 [a]	3.0[a]
	417[b]	606[b]	< 40[b]	-
7	426[a]	559[a]	213 [a]	4.2[a]
	405[b]	590[b]	112[b]	-
8	414[a]	564[a]	191[a]	4.2[a]
	408[b]	584[b]	118[b]	-
9	415[a]	594[a]	108[a]	-
	405[b]	605[b]	< 40[b]	-

[a] Dichloromethane solution. [b] Dimethylsulfoxide solution.

Cytotoxicity studies and fluorescence microscopy

The cytotoxic activity of the gold complexes **1** and **2** and the heterometallic species **4**-**9** was determined by an MTT assay in the tumor lung A549 cell line, see Table 4. All of them showed a significant mild cytotoxicity, with IC_{50} values ranging from 35 to 75 μM.[25] Such cytotoxicity was attributed to the gold fragment, as it is known that complexes of the type *fac*-[Re(bipy)$(CO)_3$(Py-derivative)]$^+$ do not normally present high antiproliferative activity.[10,26] In fact, the similar cytotoxicity values found for the gold precursors **1** and **2** and those of heterobimetallic Au(I)/Re(I) complexes **4** and **5** corroborate this result. Thus, the rhenium core is mainly lending the emissive properties to the molecule, which agrees with the cytotoxic behavior observed for other heterobimetallic Re(I)/Au(I) complexes already reported.[10] Notably, the heterotrimetallic species showed a significant increase of the cytotoxicity as all of them presented almost half IC_{50} values in comparison with that of their bimetallic precursor (Table 5). As previously suggested, the presence of a second rhenium fragment should not increase the cytotoxicity, however, it can facilitate the uptake of the probe due to a new balance between charge and lipophilicity. Casini and co-workers have also reported several gold complexes bearing a linear coordination mode of the type P-Au-P and as part of heterotrimetallic Ti-Au-Ti structures.[27] Their findings agree with the idea that the higher antiproliferative character registered for some of the trimetallic species is directly related to the different balance of lipophilicity that eases the cell uptake.[27] Moreover, it cannot be ruled out that the different coordination environment of the gold metal could affect also the antiproliferative character. Gold(I) compounds have been described to induce intracellular oxidative stress,[30] therefore, reactive oxygen species (ROS) production in A549 cells was analyzed in presence of compound **4** and **7**. After incubating both complexes with the cells for 18 hours, an oxidative stress indicator, specifically 2',7'-dichlorodihydrofluorescein diacetate (H_2-DCFDA), was added and the samples were analyzed by flow cytometry. Figure 4 and Figure S4 show that cells treated

with both complexes displayed higher DCF fluorescence, corroborating an increase in the level of intracellular ROS.

Table 4. IC_{50} (μM) values of **1**, **2**, **4** – **9** in A549 cells. Final concentration ≤ 0.5 % dimethylsulfoxide, incubation time 24 h at 37 °C.

	IC_{50}		**IC_{50}**		**IC_{50}**
1	70.32 ± 2.7	**4**	75.25±10.67	**7**	42.44 ± 4.03
2	76.33 ± 2.96	**5**	67.80 ± 4.11	**8**	36.09 ± 16.99
		6	64.69 ± 3.32	**9**	35.82 ± 1.82
Cisplatin	114.2±11[a]				

[a] Measured in H_2O at 24 h[28]

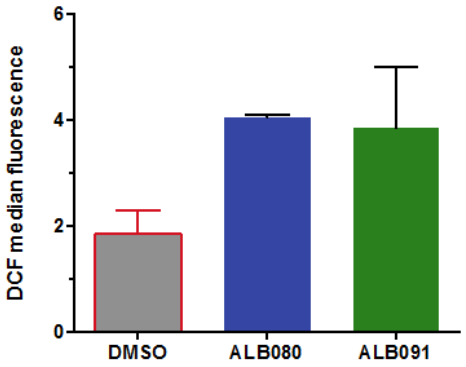

Figure 4. Histogram of DCF fluorescence of A549 cell treated with DMSO, complex 4 and 7 for 18 hours.

Fluorescence cell microscopy was used to ascertain cellular biodistribution of the different metallic species. Specifically, A549 cells were incubated with complexes **4**-**9** (25 μM final concentration) together with a commercial nuclear dye, DRAQ5, 2 μM, used as internal standard, which would be selectively visualized upon irradiation at 655 nm. After 4 h of incubation, excitation at 405 nm resulted

in the emission from samples with complexes **7** and **8**, corroborating their efficient cellular uptake and suitability for biological imaging applications, see Figure 5. Complexes **4**-**6** and **9** were not visible under those conditions, which would suggest that either they do not permeate the cell and they are eliminated during the incubation protocol, or that their emission intensity in the biological media is not strong enough to be distinguished from the autofluorescence. Besides that, quenching phenomena in biological media could not be ruled out. To further investigate the possibility of quenching due to interactions with biological material, a titration experiment was performed. Thus, increasing amounts of cysteine was added to both, a solution of compound **4** and **9**, and the luminescence intensity was examined by fluorescence spectroscopy. If the luminescence were quenched upon the addition of cysteine it would probably mean that cysteine residues have been displacing the pyridine axial ligand from the rhenium coordination sphere. It is known that S-donor ligands coordinated to Re(I) species facilitates a non-radiactive LLCT transition (from the S-donor ligand to the bisimine chelate).[26] Indeed, there is a drop of the emission intensity after the addition of one equivalent of cysteine that could indicate the presence of interaction between the probe and the aminoacid. However, even after saturation of the solution of complexes **4** and **9** with cysteine, the emission intensity remains practically the same, figure S4, implying that if interactions between the probes and the aminoacid are taken place, the gold fragment is likely to be the responsible instead of the rhenium fragment, otherwise the ^{3}MLCT transition would have been shifted or quenched. A closer look to the images from complexes **7** and **8** revealed a similar localization pattern. In both cases the emission comes from the cytoplasmic area in a non-uniform distribution. Although further analysis are needed, such pattern could be thought to be a mitochondrial localization by comparison with a) the localization found for similar cationic rhenium complexes[15,17,29] and b) the affinity of gold(I) complexes to target the thioredoxin reductase of the mitochondria.[4a,5d,31]

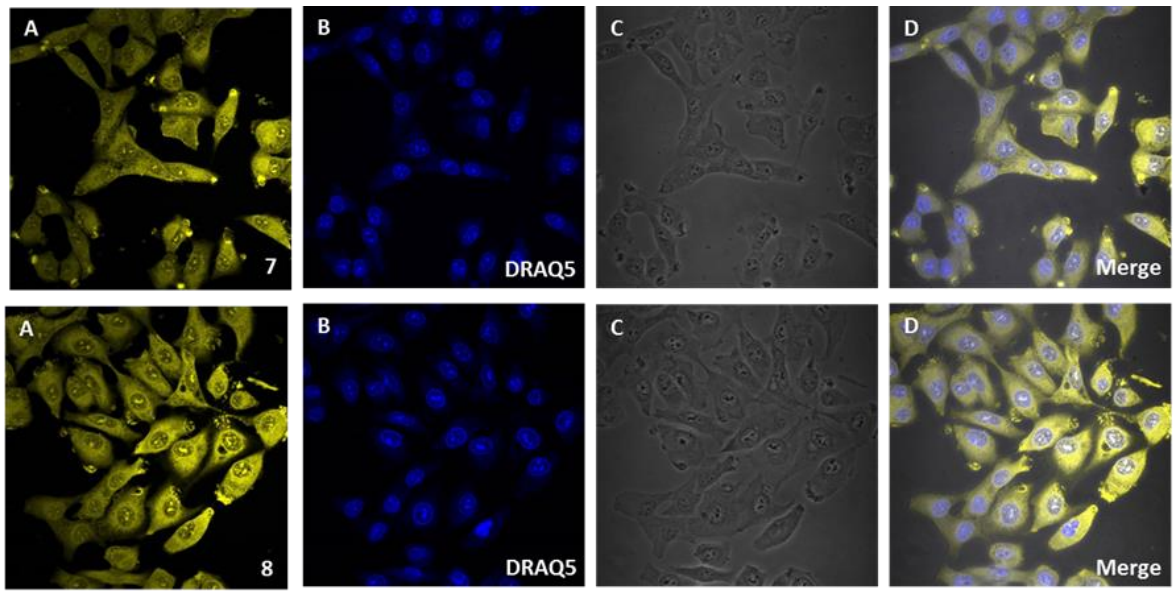

Figure 5. Images of complexes **7** and **8** incubated with A459 cells at 37 C for 4 h. (A). After irradiation at 405 nm. (B). After irradiation at 647 nm. (C) Phase contrast. (D) Superimposition image

In addition, both complexes and in particular complex **7** showed a curious localization pattern within an area close to the cell membrane (Figure 5). Thus, most of the cells presented a bright emissive dot just at the edge of the inner cell membrane upon excitation at 405 nm. The fact that the complexes seem to be retained in round spots, with a clear delimitation from the cytoplasmatic area, suggests that they are separated from the media from a physical barrier. Therefore, and considering its proximity to the cellular membrane, an endosome accumulation derived from an endocytic process seemed a plausible explanation. To examine such possibility and suppress any active transport that would evolve in endosome encapsulation, incubation of complex **8** at different concentrations at 4 °C was undertaken (Figure 6). The incubation time was reduced to 1 h in order to avoid cell death because of the low temperature. Parallel experiments at 37 °C were also undertaken for comparison purposes. In both

cases, internalization of the species was observed, pointing towards passive transport as the entry pathway and thus, discarding endosome encapsulation as consequence of endocytosis (Figure 5).

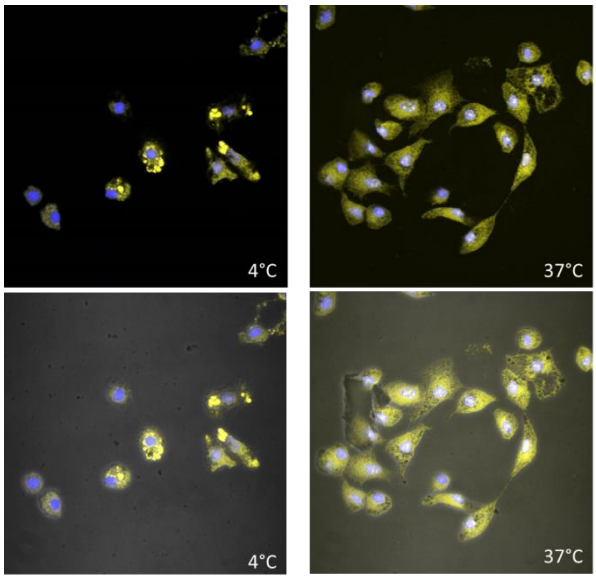

Figure 6. Complex **8** incubated with A549 cells at 4 °C and 37 °C for 1 h.

Additionally, it could be perfectly noticed as those cells incubated at 4 °C presented a peculiar droplet shape distribution pattern, which recalls these of fatty acids at high concentrations. In general, it is known that reducing the temperature will make the systems more rigid and the most stable conformation is anticipated. In this sense, complex **8** could be described as the combination of a highly hydrophilic core, entailing the metals and their immediate coordination sphere, and hydrophobic groups such as phenyls. Therefore, in a polar environment at 4 °C, its behavior might be similar to that of fatty acids, and a disposition in which there is a protection of the phenyl groups from the media might be prone to occur, simulating a micelle or an aggregate (Figures 7 and S6), i.e. the bright emissive round spots seen in Figure 6. Although the chemical structure of the metallic species is not the same, this concept goes in line with previous studies reported by Policar[32] and Coogan.[33] Both of them described

the effect of an intramolecular fold-back of the pendant alkane chain located in the axial pyridyl ligand as consequence of solvent polarity. A reversal of the effect was found at higher temperatures, recalling what has happen with complex **8** incubated for 1 h at 4 °C and 37 °C. It is also important to mention that the incubation of complex **8** performed for 1 h at 37 °C did not show any hint of the bright emissive dot just at the edge of the inner cell membrane, contrasting with the results seen for the analogous experiment performed at longer times (4 h). Therefore it is suggested that these phenomena might be time-dependent and not as consequence of the entry mechanism.

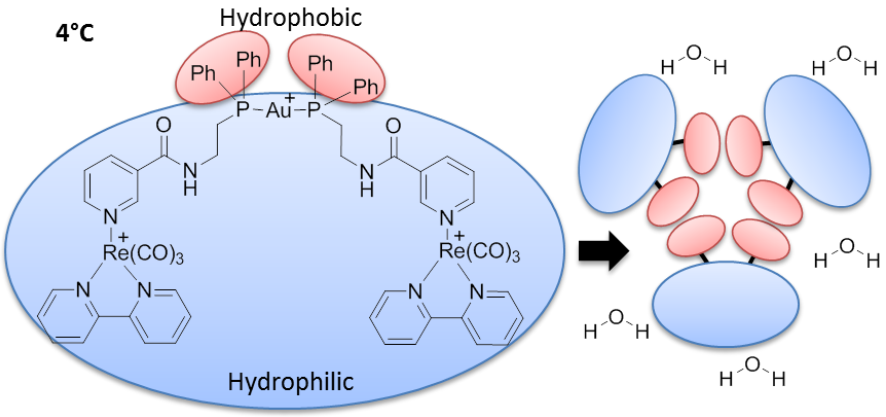

Figure 7. Proposed disposition of **8** in polar solvents at 4 °C.

Alternatively, superimposition of the images taken upon irradiation at 405 and at 655 nm revealed that there are also some strong emissive spots in the nuclear region that overlap those seen in the case of DRAQ5. As DRAQ5 is a fluorescent nuclear DNA dye, the maximum emission intensity is where the concentration of DNA is higher. Therefore, seen the consistency between the emission of complexes **7** and **8** with that of DRAQ5, DNA interaction could be suggested for those species. In fact previous reports dealing with the biodistribution of gold dervatives have already shown similar nuclear

localization. Specifically some heterometallic Re(I)/Au(I) species[10] and gold (I) N-heterocyclic carbenes[6a-6c] described by the research groups headed by Gimeno, Bodio, Rigobello and Casini revealed that these complexes have a clear preference to accumulate in this organelle. To learn more regarding such possibility, and specifically whether the trimetallic complexes reported herein interact with DNA, the reactivity of **8** with plasmid pEYFP DNA was analyzed by gel electrophoresis according to stablished procedures. The study revealed that complex **8** interacts with DNA, however it was not possible to elucidate the precise effect on it. Figure 8 clearly shows as the DNA signal disappears when combined with **8** at concentrations over $0.125 \cdot 10^{-3}$ µM. At higher concentration, the complex reverses the signal towards the anode area, possibly as consequence of their highly cationic character, and any hint of DNA pattern vanishes. This result could denote breakage of the DNA into small fragments that are eliminated from the agarose gel due to their low molecular weight, although additional studies would be needed to ascertain such a possibility. Moreover, the analogous heterobimetallic complex **5** was also tested for comparison purposes, displaying a similar behavior to that seen for **8.**

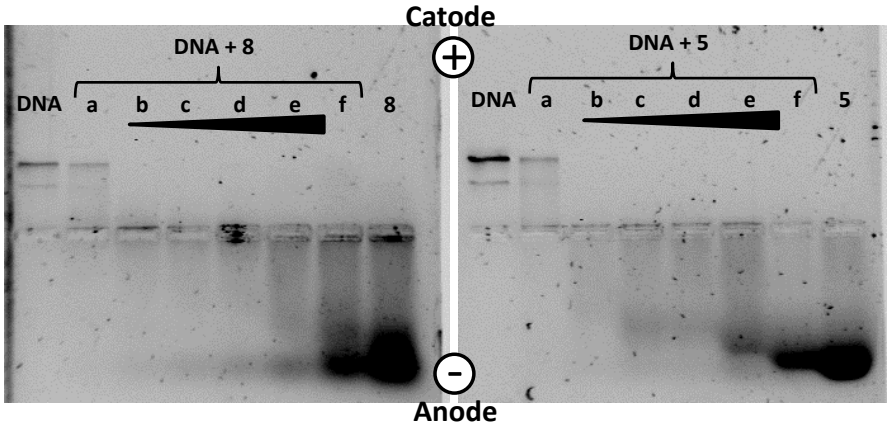

Figure 8. Gel electrophoresis of pEYFP plasmid DNA treated with different concentrations of **5** and **8**, (4.45 µM–142 µM) after 4 h incubation in PBS at 37 °C.

Another simple way to determine whether an interaction takes place between the metal complex and DNA is to examine the modifications of specific absorption bands (π-π* intraligand transitions or ligand-to-metal charge transfer) when the nucleic acid is present at different concentrations by UV spectroscopy. Thus, variation in the absorption bands of complexes upon addition of increasing amount of DNA could denote DNA intercalation (hypochromism and bathochromism or hypsochromism) or electrostatic interactions, hydrogen bonding and groove (minor or major) binding along the outside of the DNA helix (hyperchromism).[34] For that reason, DNA binding experiments were carried out by UV-absorption spectroscopy with calf-thymus DNA (CT-DNA), Figure 9 and S7. Complexes **4** and **9** were selected as models to evaluate whether the presence of the different axial ligand, either a pyridine or amine derivative, were the driving force for the DNA interaction rather than the complex itself. The hypochromism of the absorption bands together with the calculated intrinsic binding constants (K_b), $K_b = 2.77\times10^5$ and 1.14×10^5 M respectively, denote favorable interaction of the complexes with DNA, possible by intercalation. Kb values of such order of magnitude can be indicative of a relatively strong interaction between DNA and metal complexes.[35] Therefore, it can be concluded that both families of complexes show the possibility to interact with DNA, although the precise interaction is still unclear.

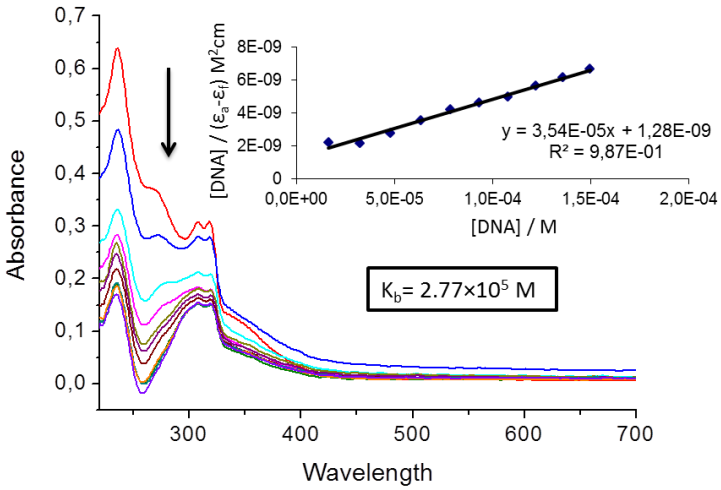

Figure 8. Absorption spectral traces of complex **4** in 0.05 M Tris-HCl buffer (pH 7.4) with increasing concentration of CT-DNA (1.7 mM) at room temperature. Inset: Figure shows plot of [DNA]/ (εa – εf) versus [DNA]

Conclusions

In summary, novel heterometallic complexes were synthesized by the combination of different metallic fragments, a luminescent Re(I) with a bioactive Au(I) derivative. A ditopic ligand, either 2-(diphenylphosphino)ethylamine (**L0**) or 2-(diphenylphosphino)ethylamidepyridine derivatives (**L1**, **L2**) was used as linkers between both metal fragments, affording three heterobimetallic and three heterotrimetallic complexes of the type *fac*-$[Re(bipy)(CO)_3(LAuCl)]^+$ (**4**-**6**) and $[(fac\text{-}[Re(bipy)(CO)_3(L)])_2Au]^{3+}$ (**7**-**9**) respectively. The use of P,N-donor ligands (L) as linkers was crucial to discriminate between both metal centers. The synthetic approach entailed an initial formation of the Au-L and L-Au-L derivatives, where L acts as a P-donor and prevented any further oxidation of the phosphine atom. Thereafter, the coordination of Au-L and and L-Au-L species to the Re luminescent fragment, *fac*-$[Re(bipy)(CO)_3(CF_3SO_3)]$ (**A**), through the nitrogen atom was performed successfully. All

of them showed an emission that was assigned to a ^{3}MLCT transition between 550 and 590 nm in dichloromethane which was red shifted up to 609 nm when measured in dimethylsulfoxide solution. Lifetimes in DMSO were in the range of 100–300 ns except for complexes **6** and **9**, which were less than 40 ns. Quantum yields measured in dichloromethane solution varies from 3 to 12.5 % and anticipates their suitability as cell imaging agents. The antiproliferative activity exhibited against A549 cancer cells was mainly due to the Au-(L0, L1, L2) fragment, with the heterobimetallic complexes being almost twice as toxic as the heterobimetallic. Interestingly, species **7** and **8** were suitable candidates for cell imaging applications using fluorescence microscopy. Both of them showed a similar behavior, they were spread around the cytoplasm in a non-uniform distribution with clear accumulation, especially in the case of compound **7**, in a single spot edge of the inner cell membrane. Incubation experiments at 4 °C showed that the complexes were able to cross the cell membrane by passive transport, discarding the bright spot of the inner cell membrane as an endosomal accumulation. Moreover, at this temperature an additional reorganization of the complex in a droplet shape pattern was observed. This effect could be the result of being highly charged species bearing hydrophobic groups such as phenyls. Additionally, both complexes displayed some DNA accumulation, which was confirmed by a colocalization experiment, using DRAQ5. Electrophoresis analysis and DNA-binding experiments by UV-absorption spectroscopy corroborates such interaction even though it was not conclusive to elucidate the precise mechanism. These preliminary results underline the potential of combining two metallic fragments with complementary properties in order to search for trackable metallodrugs. Optimal combination of luminescent metalloprobes with bioactive species would surely bring a deeper understanding on their biological interplay, which can be used in the near future for the development of the next generation of metallodrugs.

Experimental Section

General Measurements and Analysis Instrumentation

Mass spectra were recorded on a BRUKER ESQUIRE 3000 PLUS, with the electrospray (ESI) technique and on a BRUKER (MALDI-TOF). ^{1}H, $^{13}C\{^{1}H\}$ and $^{31}P\{^{1}H\}$ NMR, including 2D experiments, were recorded at room temperature on a BRUKER AVANCE 400 spectrometer (^{1}H, 400 MHz, ^{13}C, 100.6 MHz, ^{31}P, 162 MHz) with chemical shifts (δ, ppm) reported relative to the solvent peaks of the deuterated solvent. Infrared spectra were recorded in the range 4000–250 cm^{-1} on a Perkin-Elmer Spectrum 100 FTIR spectrometer. Room temperature steady-state emission and excitation spectra were recorded with a Jobin-Yvon-Horiba fluorolog FL3-11 spectrometer fitted with a JY TBX picosecond detection module. Lifetimes measurements were recorded with a LED of Horiba Jobin Ybon with pulse duration of 1.2 ns. LED frequencies were selected attending to excitations energies. Lifetime data were fitted using DAS6 V6.1 software. UV/vis spectra were recorded with a 1 cm quartz cells on an Evolution 600 spectrophotometer. The quantum yields were measured in a Hamamatsu Photonics KK.

Antiproliferative studies: MTT assay: Exponentially growing cells (A549) were seeded at a density of approximately 10^{4} cells per well in 96-well flat-bottomed microplates and allowed to attach for 24 h prior to addition of compounds. The complexes were dissolved in DMSO and added to cells in concentrations ranging from 10 to 200 μM in quadruplicate. Cells were incubated with our compounds for 24 h at 37 °C. Ten microliters of MTT (5 mg ml^{-1}) were added to each well and plates were incubated for 2 h at 37 °C. Finally, the growth media was eliminated and DMSO (100 ml per well) was

added to dissolve the formazan precipitates. The optical density was measured at 550 nm using a 96-well multiscanner autoreader (ELISA). The IC_{50} was calculated by nonlinear regression analysis.

Analysis of ROS by flow cytometry: A549 cells were seeded in 24-well plate at $5x10^5$ cells/well and allowed to attach for 10 h. Then, compound 4 and 7 were added at 25 μM in duplicate. The equivalent volumen of DMSO was added to controls. After 18 h incubation, cells were detached with a 0.25% trypsin solution, washed twice with PBS (Phosphate Buffered Saline) and resuspended in 500 μl PBS containing 10 μM H2-DCFDA (2',7'-dichlorodihydrofluorescein diacetate). Samples were incubated with this probe for 30 min at 37ºC, washed with PBS and analyzed in a flow cytometer (FacSCAN, Becton Dickinson). Data files were processed using the Weasel software.

Cell fluorescence microscopy study: European Collection of Cell Cultures, were maintained in Hepes modified minimum essential medium (DMEM) supplemented with 10% fetal bovine serum, penicillin, and streptomycin. A549 cells were detached from the plastic flask using trypsin-EDTA solution and suspended in an excess volume of growth medium. The homogeneous cell suspension was then distributed into 24-well flat-bottomed microplates over a cover slip placed inside each well and they were allowed to attach for 24 h prior to addition of compounds. Complexes were added (10 μl) to the cells up to a final concentration of 25 μM. After incubation for 4 h at 37 °C, the growth medium was removed and 0.5 ml of PBS was added for a washing step (3 times). Thereafter, 0.5 ml of paraformaldehyde (4%) was added and allowed to stand for 15 min at room temperature. Eventually the paraformaldehyde was removed and further washings with PBS were performed (3 × 0.5 ml). The cover slips were collected from the 24 well plate, immersed for 1 or 2 seconds in distilled water and let them to drip the water. Then, they are placed over a microscope slide where a drop of fluoromont with 2 μM

DRAQ5 was previously placed. Preparations were viewed using an Olympus FV10-i Oil type compact confocal laser microscope using a ×10 or ×60 objective, with excitation wavelength at 405 and 650 nm.

DNA interaction assay: First, 20 μl aliquots of pEYFP plasmid DNA (5 ng/ml) in buffer Tris-acetate/EDTA buffer (TAE) were incubated with different concentrations of the compounds 5 and 8 (4.45 μM – 142 μM) at 37 °C for 4 h in the dark. Samples of free DNA were prepared as controls. After the incubation period, the samples were loaded onto 0.8 % agarose gel containing SyBr-SAFE stain. The samples were separated by electrophoresis for 30 min at 90 V in Tris-acetate/EDTA buffer (TAE). Afterwards, the gel was visualized in a GelDoc (BioRad).

Absorption Spectral Studies. DNA binding experiments were carried out in Tris-HCl buffer 0.05 M pH 7.4) using a DMSO solution of the complex. The concentration Calf thymus DNA (CT-DNA) was determined from its absorbance intensity at 260 nm and its known molar absorption coefficient value 6600 M^{-1} cm^{-1}.[35] Absorption spectral titration experiments were performed by varying the concentration of CT-DNA while keeping the complex concentration constant. Before each measurement sample were equilibrated with CT-DNA for 10 min. The absorbance of the complex was measured after each successive addition of CT-DNA. The intrinsic DNA binding constant (K_b) was obtained using the equation:$[DNA]/(\varepsilon_a - \varepsilon_f) = [DNA]/(\varepsilon_b - \varepsilon_f) + 1/K_b(\varepsilon_a - \varepsilon_f)$ where [DNA] is the concentration of DNA in the base pairs, ε_a is the apparent extinction coefficient observed for the complex, ε_f corresponds to the extinction coefficient of the complex in its free form, and ε_b refers to the extinction coefficient of the complex when fully bound to DNA.[37] $[DNA]/(\varepsilon_a - \varepsilon_f)$ vs. [DNA] were plotted and the ratio of the slope to intercept from the linear fit gives the value of the intrinsic binding constant (K_b).

Materials and Procedures

The starting material [AuCl(tht)][38] and [Re(bipy)(CO)$_3$(OTf)][39] were prepared according to literature procedures. Compound **3** was synthesized using a similar procedure from the one previously described in the literature.[40] All other starting materials, including **L0**, and solvents were purchased from commercial suppliers and used as received unless otherwise stated.

Synthesis of L1. To a stirred solution of diphenylphosphinoethylamine (539.3 mg, 2.24 mmol) in CH_2Cl_2 (20 ml) was added isonicotinoylchloride hydrochloride (410.6 mg, 2.24 mmol) followed by Et_3N (0.624 mL, 4.48 mmol) dropwise. The solution was allowed to stir for two days at room temperature under argon atmosphere, while its colour changed from red to yellowish. The reaction was stopped by addition of saturated aqueous $NaHCO_3$ (20 mL) and the organic phase was washed again with saturated aqueous $NaHCO_3$ (20 mL). The aqueous layers were combined and extracted with CH_2Cl_2 (3 × 20 mL). The combined extracts were washed with brine (40 mL), dried over anhydrous Na_2SO_4, filtered and concentrated to afford a crude mixture. The crude was purified by silica gel column chromatography using ethyl acetate:hexane (8:2 to 9:1) as eluent to afford an orange oil containing compound **L1** with ca. 12 % wt of the corresponding oxide (528.8 mg, 62 %). ^{1}H NMR (CD_2Cl_2, 400 MHz): δ 8.65 (dd, *J* = 4.4, 1.7 Hz, 2H, H_1), 7.41 (dd, *J* = 4.4, 1.7 Hz, 2H, H_1), 7.49-7.44 (m, 4H, *o*-H, Ph) 7.37-7.32 (m, 6H, *m*-H+*p*-H, Ph), 6.39 (s, br, 1H, NH), 3.62 (dtd, *J* = 11.2, 7.2, 5.8 Hz, 2H, H_6), 2.43 (t_{ap}, *J* = 7.2 Hz, 2H, H_5). ^{31}P NMR (CD_2Cl_2, 162 MHz): δ -20.8 (s, 1P). ^{13}C NMR (CD_2Cl_2, 101 MHz): δ 150.9 (s, C_1), 133.25 (d, $^3J_{P\text{-}C}$ = 19.1 Hz, *m*-C, Ph), 131.1 (d, $^4J_{P\text{-}C}$ = 9.6 Hz, *p*-C, Ph), 129.4 (d, $^2J_{P\text{-}C}$ = 23.7 Hz, *o*-C, Ph), 129.2 (s, C_2), 38.2 (d, $^1J_{P\text{-}C}$ = 20.7 Hz, C_6), 28.7 (d, $^2J_{P\text{-}C}$ = 13.6 Hz, C_5). IR (cm^{-1}): 3349 υ(NH), 3048 υ(C_{Ar}-H), 1642 υ(N-C=O), 1541 υ(NH δ).

Synthesis of L2. This compound was prepared similarly to **L1** using nicotinoyl chloride hydrochloride instead of isonicotinoyl chloride hydrochloride. **L2** was obtained as an orange oil (419.5 mg, 48 %) and

once again with a 12%wt unpurified with the corresponding oxide. ^{1}H NMR (CD_2Cl_2, 400 MHz): δ 8.78 (dd, *J* = 2.3, 0.8 Hz, 1H, H_5), 8.67 (dd, *J* = 4.8, 1.7 Hz, 1H, H_1), 7.90 (ddd, *J* = 7.9, 2.3, 1.8 Hz, 1H, H_3), 7.50-7.45 (m, 4H, H_{10}), 7.37-7.32 (m, 7H, H_{11}+H_{12}+H_2), 6.34 (s, br, 1H, NH), 3.66-3.57 (m, 2H, H_8), 2.46-2.41 (m, 2H, H_7). ^{31}P NMR (CD_2Cl_2, 162 MHz): δ -20.8 (s, 1P). ^{13}C NMR (CD_2Cl_2, 101 MHz): δ 165.7 (s, C_6), 152.4 (s, C_5), 148.5 (s, C_1), 138.4 (d, $^{1}J_{P\text{-}C}$= 12.6 Hz, C_{ipso}, Ph), 135.1 (s, C_3), 133.1 (d, $^{2}J_{P\text{-}C}$ = 19.0 Hz, *o*-C, Ph), 130.6 (s, C_4), 129.2 (s, *p*-C, Ph), 129.0 (d, $^{3}J_{P\text{-}C}$ = 6.8 Hz, *m*-C, Ph), 123.7 (s, C_2), 37.9 (d, $^{1}J_{P\text{-}C}$ = 21.2 Hz, C_8), 28.6 (d, $^{2}J_{P\text{-}C}$ = 13.4 Hz, C_7). IR (cm^{-1}): 3265 υ(NH), 3069 υ(C_{Ar}-H), 1630 υ(N-C=O), 1554 υ(NH δ).

Synthesis of 1. To a stirred solution of **3** (200 mg, 0.433 mmol) in DCM (10 mL) was added isonicotinoyl chloride hydrochloride (324.8 mg, 1.73 mmol) followed by Et_3N (722 µL, 5.20 mmol) and the resulting solution was allowed to react overnight. The reaction was quenched by the addition of water (20 mL) and the organic layer was separated and further washed with a saturated aqueous solution of $NaHCO_3$ (2 x 20 mL), dried over anhydrous Na_2SO_4, filtrated and evaporated. The crude product was purified by alumina column chromatography using MeOH/CH_2Cl_2 (2:98). The desired compound was obtained as a white solid (226.8 mg, 92 %). ^{1}H NMR (CD_2Cl_2, 400 MHz): δ 8.67 (d_{ap}, *J* = 5.0 Hz, 2H, H_1), 7.79-7.70 (m, 4H, *o*-H, Ph), 7.53-7.45 (m, 8H, *m*-H+*p*-H+H_2), 6.68 (s, br, 1H, NH), 3.85-3.73 (m, 2H, H_5), 2.93 (dt, *J* = 10.7, 6.5 Hz, 2H, H_6). ^{31}P NMR (CD_2Cl_2, 162 MHz): δ 24.8 (s, 1P). ^{13}C NMR (CD_2Cl_2, 101 MHz): δ 166.1 (s, C_4), 151.02 (s, C_1), 133.8 (d, $^{2}J_{P\text{-}C}$ = 13.3 Hz, *o*-C, Ph), 132.8 (d, $^{4}J_{P\text{-}C}$ = 2.6 Hz, *p*-C, Ph), 130.0 (d, $^{3}J_{P\text{-}C}$ = 11.7 Hz, *m*-C, Ph), 129.4 (d, $^{1}J_{P\text{-}C}$ = 61.2 Hz, *ipso*-C, Ph), 121.4 (s, C_2), 37.4 (d, $^{2}J_{P\text{-}C}$ = 5.2 Hz, C_5), 28.5 (d, $^{1}J_{P\text{-}C}$ = 38.2 Hz, C_6). IR (cm^{-1}): 3313 υ(NH), 3054 υ(C_{Ar}-H), 1663 υ(N-C=O), 1553 υ(NH δ), 325 υ(Au-Cl). HRMS (m/z): 589.0458 (M^+) $C_{20}H_{19}AuClN_2O_2P_2$ (589.0481).

Synthesis of 2. This compound was prepared similarly to **1** but using nicotinoyl chloride hydrochloride instead of isonicotinoyl chloride hydrochloride. Compound **2** was obtained as a white solid (212 mg, 86%). ^{1}H NMR (CD_2Cl_2, 400 MHz): δ 8.82 (d, *J* = 1.8 Hz, 1H, H_5), 8.67 (dd, *J* = 4.8, 1.6 Hz, 1H, H_1), 7.96 (ddd, *J* = 8.0, 2.2, 1.8 Hz, 1H, H_3), 7.69-7.61 (m, 4H, *o*-H, Ph), 7.46-7.36 (m, 6H, *m*-H+*p*-H), 7.34 (ddd, *J* = 7.9, 4.8, 0.8 Hz, 1H, H_2), 6.70 (t, *J* = 5.0 Hz, 1H, NH), 3.79 (dc_{ap}, *J* = 15.5, 6.7 Hz, 2H, H_8), 2.95 (dt, *J* = 10.9, 6.8 Hz, 2H, H_7). ^{31}P NMR (CD_2Cl_2, 162 MHz): δ 24.8 (s, 1P). ^{13}C NMR (101 MHz, chloroform-*d*) δ 166.09 (s, C_6), 152.34 (s, C_5), 148.5 (s, C_1), 135.2 (s, C_3), 133.3 (d, $^{2}J_{P\text{-}C}$= 13.3 Hz, *o*-C, Ph), 132.2 (d, $^{4}J_{P\text{-}C}$ = 2.6 Hz, *p*-C, Ph), 129.5 (d, $^{3}J_{P\text{-}C}$ = 11.8 Hz, *m*-C, Ph), 128.4 (s, C_4), 128.8 (d, $^{1}J_{P\text{-}C}$ = 61.3 Hz, *ipso*-C, Ph), 123.5 (s, C_2), 37.1 (d, $^{2}J_{P\text{-}C}$ = 5.1 Hz, C_7), 28.1 (d, $^{1}J_{P\text{-}C}$ = 38.0 Hz, C_8). IR (cm^{-1}): 3316 υ(NH), 3049 υ(C_{Ar}-H), 1643 υ(N-C=O), 1529 υ(NH δ), 689 υ(P-C), 318 υ(Au-Cl). HRMS (m/z): 567.0697 [$M+H^+$] $C_{20}H_{20}AuClN_2O_2P$ (567.0662).

Synthesis of 3. [40] To a stirred solution of (diphenylphosphino)ethylamine (429.6 mg, 1.78 mmol) in CH_2Cl_2 (5 mL) was added [AuCl(tht)] (571.1 mg, 1.78 mmol) and the reaction mixture was allowed to stir for 1.5 h at room temperature under argon atmosphere. The solution was then concentrated and ether was added to afford an oily solid. The solid was dissolved in DCM and precipitated again with ether affording **3** as a white solid (636.6 mg, 86%). ^{1}H NMR (CD_2Cl_2, 400 MHz): δ 7.81-7.69 (m, 4H, H_4), 7.56-7.43 (m, 6H, H_5+H_6), 3.10-2.99 (m, 2H, H_2), 2.85-2.76 (m, 2H, H_1). ^{31}P NMR (CD_2Cl_2, 162 MHz): δ 28.7 (s, 1P). ^{13}C NMR (101 MHz, CD_2Cl_2): δ 133.8 (d, $^{2}J_{P\text{-}C}$ = 13.2 Hz, *o*-C, Ph), 132.2 (d, *p*-C, Ph), 130.5 (d, $^{1}J_{P\text{-}C}$ = 55.4 Hz, *ipso*-C, Ph), 129.7 (d, $^{3}J_{P\text{-}C}$ = 11.1 Hz, *m*-C, Ph), 38.5 (d, $^{2}J_{P\text{-}C}$ = 5.3 Hz, C_1), 32.1 (d, $^{1}J_{P\text{-}C}$ = 35.2 Hz, C_2). IR (cm^{-1}): 3256 υ(NH), 3049 υ(C_{Ar}-H), 322 υ(Au-Cl).

Synthesis of 4. To a stirred solution of **1** (1eq, 117 mg, 0.207 mmol) in DCM (15 mL) was added **A** (2 eq, 238.1 mg, 0.414 mmol). The reaction was stopped after 20 h when black particles of decomposed

gold appeared. The solution was filtrated by celite, evaporated and purified by alumina column chromatography using MeOH/CH_2Cl_2 (9: 1) to (97:3) as eluents. (51.5 mg, 22%). ^{1}H NMR (400 MHz, methylene chloride-d_2) δ 9.74 (t, J = 5.6 Hz, 1H, NH), 9.17 (ddd, J = 5.5, 1.6, 0.7 Hz, 2H, H_6), 8.45 (d, J = 8.3 Hz, 1H, H_3), 8.27–8.21 (m, 4H, H_4+H_7), 8.08 (d_{ap}, J = 5.2, 1.5 Hz, 2H, H_8), 7.78 (ddd, J = 7.7, 5.5, 1.3 Hz, 2H, H_5), 7.73 – 7.62 (m, 4H, *o*-H, Ph), 7.49–7.36 (m, 6H, *m*-H+*p*-H, Ph), 3.67 – 3.56 (m, 2H, H_{11}), 2.99 (dt, J = 10.8, 7.0 Hz, 2H, H_{12}). ^{31}P NMR (162 MHz, CD_2Cl_2) δ 22.65 (s). ^{13}C NMR (101 MHz, methylene chloride-d_2) δ 196.0 (s, 2CO), 191.6 (s, CO), 163.3 (s, C_{10}), 156.2 (s, C_2), 153.7 (s, C_6), 152.4 (s, C_4 or C_8), 144.6 (s, C_9), 141.8 (s, C_4 or C_8), 133.9 (d, $^2J_{P\text{-}C}$ = 13.3 Hz, *o*-C, Ph), 132.4 (d, $^4J_{P\text{-}C}$ = 2.6 Hz, *p*-C, Ph), 129.7 (d, $^3J_{P\text{-}C}$ = 11.7 Hz, *m*-C, Ph), 129.6 (s, C_5), 129.6 (d, $^1J_{P\text{-}C}$ = 61.0 Hz, *ipso*-C, Ph), 125.9 (s, C_7), 125.6 (s, C_3), 36.2 (d, $^2J_{P\text{-}C}$ = 5.5 Hz, C_{11}), 28.0 (d, $^1J_{P\text{-}C}$ = 37.8 Hz, C_{12}) IR (cm^{-1}): 3200 υ(NH), 3058 υ(C_{Ar}-H), 2028, 1905 υ(CO), 1660 υ(N-C=O), 1602 υ(C=N), 320 υ(Au-Cl). HRMS (m/z): 993.0643 $[M\text{-}OTf]^+$ $C_{33}H_{27}AuClN_4O_4PRe$ (993.0668).

Synthesis of 5. To a stirred solution of [Re(bipy)$(CO)_3$(OTf)] (**A**) (92.2 mg, 0.160 mmol) in dry CH_2Cl_2 was added **2** (90.8 mg, 0.160 mmol) and the reaction mixture was allowed to stir for two days at rt until the apparition of black particles corresponding to decomposed gold. The suspension was filtered over celite and concentrated to afford a crude which was purified by alumina column chromatography using MeOH/CH_2Cl_2 (1:40 to 4:40). Compound **5** was obtained as a yellow solid (65.5mg, 36%). ^{1}H NMR (CD_2Cl_2, 400 MHz): δ 9.20-9.17 (m, 2H, H_6), 8.89 (t, J = 5.1 Hz, 1H, NH), 8.57 (d_{ap}, J = 1.3 Hz 1H, H_{11}), 8.53 (d, J = 7.8 Hz, 1H, H_9), 8.44 (d, J = 8.1 Hz, 2H, H_3), 8.32 (d, J = 5.2 Hz, 1H, H_7), 8.14 (t, J = 7.5 Hz, 2H, H_4), 7.78 (dd, J = 7.1, 5.9 Hz, 2H, H_5), 7.70-7.63 (m, 4H, *o*-H, Ph), 7.48-7.43 (m, 6H, *m*-H+*p*-H, Ph), 7.33 (dd, J = 7.5, 5.9 Hz, 1H, H_8), 3.63 (dt, J = 20.3, 6.4 Hz, 2H, H_{13}), 2.92 (dt, J = 10.6, 7.0 Hz, 2H, H_{14}). ^{31}P NMR (CD_2Cl_2, 162 MHz): δ 20.8 (s, 1P). ^{13}C NMR (CD_2Cl_2, 101 MHz): δ 195.1

(CO), 162.9 (s, C_{12}), 155.9 (s, C_2), 153.6 (s, C_6), 151.2 (s, C_{11}), 141.2 (s, C_4), 139.4 (s, C_9), 133.4 (d, $^2J_{P-C}$ = 13.2 Hz, *o*-C, Ph), 132.1 (d, $^4J_{P-C}$ = 2.5 Hz, *p*-C, Ph), 129.4 (d, $^3J_{P-C}$ = 11.7 Hz, *m*-C, Ph), 129.3 (s, C_{10}), 129.0 (d, $^1J_{P-C}$ = 61.2 Hz, *ipso*-C, Ph), 126.6 (s, C_8), 125.4 (s, C_3), 35.5 (d, *J* = 5.0 Hz, C_{13}), 27.90 (d, *J* = 37.8 Hz, C_{14}). IR (cm^{-1}): 3313 υ(NH), 3056 υ(C_{Ar}-H), 2029, 1904 υ(CO), 1662 υ(N-C=O), 1603 υ(C=N), 322 υ(Au-Cl) HRMS (m/z): 993.0671 ($[M\text{-}OTf]^+$), $C_{33}H_{27}AuClN_4O_4PRe$ (993.0668).

Synthesis of 7 and 8. To a stirred solution of the bisphophine-gold compound **10** or **11** (0.62 mg, 0.06 mmol) in DCM was added A (0.68 mg, 0.12 mmol). The reaction was followed by RMN and stopped when no evolution was observed. The crude mixture was evaporated and purified by alumina column chromatography using MeOH/CH_2Cl_2 (2:98 to 4:96). Complex **7** and **8** were obtained as yellow solids (51.5 mg, 50%) and (35.7 mg, 18 %) respectively. (**7**) ^{1}H NMR (400 MHz, CD_2Cl_2) δ 10.06 (t, *J* = 5.1 Hz, 1H, NH), 9.19 (dd, *J* = 5.5, 0.9 Hz, 2H, H_6), 8.74 (d, *J* = 8.1 Hz, 2H, H_3), 8.30 (td, *J* = 8.0, 1.5 Hz, 2H, H_4), 8.18 (m, 2H, H_7), 7.93 (m, 2H, H_8), 7.82 (ddd, *J* = 7.8, 5.6, 0.9 Hz, 2H, H_5), 7.75-7.68 (m, 4H, *o*-H, Ph), 7.35-7.28 (m, 6H, *m*-H_+ *p*-H, Ph), 3.76-3.65 (m, 2H, H_{11}), 3.08 (t, *J* = 6.2 Hz, 2H). ^{31}P NMR (CD_2Cl_2, 162 MHz): δ 34.5 (s, 1P). ^{13}C NMR (75 MHz, $CDCl_3$) δ 195.5 (s, 2CO), 190.9 (s, CO), 162.8 (s, C_{10}), 155.8 (s, C_2), 152.9 (s, C_6), 151.8 (s, C_7), 143.8 (s, C_9), 141.9 (s, C_4), 133.4 (s, *o*-C, Ph), 131.5 (s, *p*-C, Ph), 129.9 (s, *ipso*-C, Ph), 129.3 (s, *m*-C, Ph), 129.2 (s, C_5), 126.4 (s, C_3), 125.3 (s, C_8), 37.0 (s, C_{11}), 27.6 (s, C_{12}). HRMS (m/z): 761.1339 [M-Au]/2, $C_{33}H_{27}N_4O_4PRe$ (761.1323), 993.0698 [M-Au]/2+AuCl, $C_{33}H_{27}AuClN_4O_4PRe$ (993.0668). IR (cm^{-1}): 3054 υ(C_{Ar}-H), 2027, 1902 υ(CO), 1660 υ(N-C=O),1602 υ(C=N), 1542 υ(NH δ). (**8**) ^{1}H NMR (400 MHz, $CDCl_3$) δ 9.66 (t, *J* = 5.3 Hz, 1H, NH), 9.25 (d, *J* = 5.2 Hz, 2H, H_2), 8.73 (d, *J* = 7.3 Hz, 2H, H_5), 8.64 (s, 1H, H_{11}), 8.42 (d, *J* = 7.3 Hz, 1H, H_7), 8.25 (t, *J* = 7.6 Hz, 2H, H_4), 8.20 (d, *J* = 5.3 Hz, 1H, H_9), 7.78 (dd, *J* = 7.6, 5.2 Hz, 2H, H_3), 7.73-7.65 (m, 4H, *o*-H, Ph), 7.35-7.23 (m, 7H, *m*-H+ *p*-H+H_8), 3.88-3.75 (m, 2H, H_{13}), 3.16-3.06 (m,

2H, H_{14}). ^{31}P NMR (CD_2Cl_2, 400 MHz): δ 34.54 (s, 1P). MS (m/z): 993.3 $(M/2+Cl)^+$, 865.4 $(M-2[Re])^+$, 777.3 $(M/2-Au+O)^+$, 761.3 $(M/2-Au)^+$. ^{13}C NMR (101 MHz, CDCl3) δ 195.2 (s, 2CO), 190.9 (s, CO), 162.6 (s, C_{12}), 155.7 (s, C_2), 153.4 (s, C_6), 153.0 (s, C_9), 151.6 (s, C_{11}), 141.7 (s, C_4), 138.9 (s, C_7), 133.4 (s, *o*-C, Ph), 132.0 (s, C_{10}), 131.6 (s, *ipso*-C, Ph), 129.4 (s, *m*-C, Ph), 129.2 (s, C_5), 126.4 (s, C_8), 125.8 (s, C_3), 37.2 (s, C_{13}), 27.7 (s, C_{14}). J_{P-C} not observed. IR (cm^{-1}): 3187 υ(NH), 3049 υ(C_{Ar}-H), 2028, 1904 υ(CO), 1659 υ(N-C=O), 1603 υ(C=N), 1538 υ(NH δ).

Synthesis of 6 and 9. To a solution of **3** (40 mg, 0.087 mmol) in CH_2Cl_2 (10 mL) was added **A** (99.8 mg, 0.174 mmol) and the reaction mixture was stirred overnight. After 36 h of stirring at room temperature, the mixture was filtered over celite and concentrated to vacuo. The crude was purified by alumina chromatography using a mixture of MeOH:CH_2Cl_2 (from 1.5:100 to 6:100). Compound **6** and **9** were obtained as yellow solids (32.1 mg, 38% and 42 mg, 47% respectively). (**6**) ^1H NMR (400 MHz, CD_2Cl_2): δ 9.00 (dd, *J* = 5.5, 0.8 Hz, 2H, H_6), 8.36 (d, *J* = 8.2 Hz, 2H, H_3), 8.13 (td, *J* = 8.0, 1.5 Hz, 2H, H_4), 7.70-7.62 (m, 4H, *o*-H, Ph), 7.59 (ddd, *J* = 7.6, 5.5, 1.2 Hz, 2H, H_5), 7.54-7.47 (m, 2H, *p*-H, Ph), 7.47-7.41 (m, 4H, *m*-H, Ph), 4.57 (t, *J* = 7.0 Hz, 2H, NH_2), 3.02-2.93 (m, 2H, H_7), 2.87-2.75 (m, 2H, H_8). ^{31}P NMR (CD_2Cl_2, 162 MHz): δ 23.6 (s, 1P). IR(cm^{-1}): 3229 υ(NH), 3024 υ(C_{Ar}-H), 2021, 1894 υ(CO), 1603 υ(C=N), 322 υ(Au-Cl). HRMS (m/z): 888.0443 [M-OTf] $[Re(bipy)(CO)_3NH_2(CH_2)_2PPh_2AuCl]^+$ (888.0453). (**9**) ^1H NMR (400 MHz, CD_2Cl_2): δ 8.92 (dd, *J* = 5.4, 0.8 Hz, 2H, H_6), 8.37 (d, *J* = 8.1 Hz, 2H, H_3), 8.07 (td, *J* = 8.0, 1.4 Hz, 2H, H_4), 7.67 (d, *J* = 7.0 Hz, 4H, *o*-H, Ph), 7.54-7.41 (m, 8H, H_5+m-H+p-H), 3.12-3.03 (m, 4H, H_7), 3.03-2.93 (m, 4H, H_8). ^{31}P NMR (CD_2Cl_2, 162 MHz): δ 34.9 (s, 1P). ^{13}C NMR (101 MHz, $CDCl_3$) δ 156.0 (s, C_2), 154.1 (s, C_6), 140.5 (s, C_4), 133.4 (s, *o*-C, Ph), 132.1 (s, *p*-C, Ph), 129.7 (s, *m*-C, Ph), 128.1 (s, C_5), 124.5 (s, C_3), 46.5 (s, C_7), 30.0 (s, C_8). δCO and J_{P-C} not observed IR (cm^{-1}): 3233 υ(NH), 3054 υ(C_{Ar}-H), 2021, 1894

υ(CO), 1603 υ(C=N). MS (m/z): 656.2 ($[Re(bipy)(CO)_3NH_2(CH_2)_2PPh_2]^+$), 655.2 ($(Au[NH_2(CH_2)_2PPh_2]_2)^+$, 541.1 ($[Re[(bipy)(CO)_3NH_2(CH_2)_2PPh_2]_2Au]^{2+}$). HRMS (m/z): 888.0433 ([M-Au]/2)+AuCl ($C_{27}H_{24}AuClN_3O_3PRe$: 888.0453), 656.1145 ([M-Au]/2) ($C_{27}H_{24}N_3O_3PRe$: 656.1108).

Synthesis of 10. To a stirred solution of $[Au(tmbn)_2]OTf$ in DCM (20 mL) was added isonicotinoyl chloride hydrochloride (151.5 mg, 0.809 mmol) followed by Et_3N (1.214 mmol, 1.69 µL). The reaction was quenched one night after by the addition of a saturated aqueous solution of $NaHCO_3$ (30 mL). The organic layer was separated and washed again with $NaHCO_3$ (aq) (30 mL) and water (20 mL), dried over anhydrous Na_2SO_4, filtrated and evaporated. The crude mixture was purified by alumina column chromatography using $MeOH/CH_2Cl_2$ (97:3) as eluent. Compound **10** was obtained as a white solid (90.8 mg, 82 %) ^{1}H NMR (400 MHz, CD_2Cl_2) δ 9.10 (s, 1H, NH), 8.61 (dd_{ap}, J = 4.5, 1.6 Hz, 2H, H_1), 7.73 (dd_{ap}, J = 4.4, 1.6 Hz, 2H, H_2), 7.68 – 7.60 (m, 4H, *o*-H, Ph), 7.41 – 7.30 (m, 6H, *m*-H+*p*-H, Ph), 3.93–3.77 (m, 2H, H_5), 3.11–2.98 (m, 2H, H_6). ^{13}C NMR (101 MHz, chloroform-*d*) δ 165.6 (s, C_4) 150.2 (s, C_1), 140.3 (s, C_3), 133.0 (d, $^3J_{P-C}$ = 13.0 Hz, *m*-C, Ph) 131.5 (s, C_{10}), 130.4 (d, $^1J_{P-C}$ = 47.7 Hz, *ipso*-C, Ph), 129.2 (d, $^4J_{P-C}$ = 9.8 Hz, *p*-C, Ph), 121.4 (s, C_2), 36.9 (s, C_5), 27.9 (d, $^2J_{P-C}$ = 28.0 Hz, *o*-C, Ph). ^{31}P NMR (162 MHz, $CDCl_3$) δ 32.39 (s_{br}). IR (cm^{-1}): 3222 υ(NH), 3043 υ(C_{Ar}-H), 1660 υ(N-C=O), 1529 υ(NH δ). HRMS (m/z): 865.2123 [M-SbF_6], $C_{40}H_{38}AuN_4O_2P_2$ (865.2130).

Synthesis of 11. This compound was prepared similarly to **10** using nicotinoyl chloride hydrochloride instead of isonicotinoyl chloride. Compound **11** was obtained as a white solid (15.5 mg, 54%). ^{1}H NMR (400 MHz, methylene chloride-d_2) δ 9.45 (s_{br}, 1H, NH), 9.05 (dd, J = 2.3, 0.7 Hz, 1H, H_5), 8.58 (dd, J = 4.8, 1.7 Hz, 1H, H_1), 8.19 (ddd, J = 7.9, 2.3, 1.7 Hz, 1H, H_3), 7.72 (d, J = 6.2 Hz, 4H, *o*-H, Ph), 7.41 –

7.31 (m, 6H, *m*-H+*p*-H, Ph), 7.22 (ddd, *J* = 7.9, 4.8, 0.9 Hz, 1H, H_2), 3.83 (s, br, 2H, H_7), 3.13 (t_{ap}, *J* = 6.0 Hz, 2H, H_8). ^{31}P NMR (162 MHz, CD_2Cl_2) δ 36.17. ^{13}C NMR (75 MHz, $CDCl_3$) δ 166.1 (s, C_6), 151.9 (s, C_5), 149.6 (s, C_1), 135.3 (s, C_3), 133.3 (s, *o*-C, Ph), 131.7 (s, *p*-C, Ph), 130.0 (s, *ipso*-C, Ph), 129.4 (s, *m*-C, Ph), 129.1 (s, C_4), 123.0 (s, C_2), 36.7 (s, C_7), 28.1 (s, C_8). IR (cm^{-1}): 3220 υ(NH), 3050 υ(C_{Ar}-H), 1646 υ(N-C=O), 1590 υ(C=N), 1534 υ(NH δ). HRMS (m/z): 865.2208 [M-SbF_6], $C_{40}H_{38}AuN_4O_2P_2$ (865.2130).

ASSOCIATED CONTENT

Supporting Information includes:

Table of chemical shift of L1-L2 and 1-3 in $^{31}P\{^1H\}$ NMR in CD_2Cl_2, Figures of a) UV-visible spectra of 4-8 in dlchloromethane, b) Normalized emission spectra of **4** – **8** in dimethyl sulfoxide, c) Normalized emission spectra of **4** and **9** in a mixture of DMSO and PBS (pH = 7.4, ≤0.5 % DMSO), d) Histograms collected from a flow cytometry experiment of A549 cells treated with compound **4** and **7** for 18h and later with a fluorescent ROS indicator (2',7'-dichlorodihydrofluorescein diacetate (H_2-DCFDA), e) Titration experiment of complexes **4** and **9** in DMSO with increasing amount of cysteine, F) Proposed disposition of **8** in polar solvents at 4 °C and at 37 °C, g) Absorption spectral traces of **9** complex in 0.05M Tris-HCl buffer (pH 7.4) with increasing concentration of CT-DNA.

AUTHOR INFORMATION

Corresponding Author

*email: vanesa@unizar.es

*email: gimeno@unizar.es

Orcid

Vanesa Fernández-Moreira: 0000-0002-1218-7218

M. Concepción Gimeno Floría:FALTA TU ORCID

Author Contributions

The manuscript was written through contributions of all authors. All authors have given approval to the final version of the manuscript.

Funding Sources

The authors thank the Ministerio de Economía y Competitividad (MINECO-FEDER CTQ2016-75816-C2-1-P and CTQ2015-70371-REDT) and Gobierno de Aragón-Fondo Social Europeo (E77) for financial support.

REFERENCES

(1) Bertrand, B.; Doulain, P.-E.; Goze, C.; Bodio, E. Development of Trackable Metal-Based Drugs: New Generation of Therapeutic Agents. *Dalton Trans.* **2016**, *45*, 13005–13011.

(2) Ward, J. R.; Williams, H. J.; Egger, M. J.; Reading, J. C.; Boyce, E.; Altz-Smith, M.; Samuelson Jr., C. O.; Willkens, R. F.; Solsky, M. A.; Hayes, S. P.; Blocka, K. L.; Weinstein, A.; Meenan, R. F.; Guttadauria, M.; Kaplan, S. B.; Klippel, J. Comparison of Auranofin, Gold Sodium

Thiomalate, and Placebo in the Treatment of Rheumatoid Arthritis. *Arthritis Rheum.* **1983**, *26*, 1303–1315.

(3) For clinical trial in progress of auranofin: https://clinicaltrials.gov/ct2/show/NCT01737502 For clinical trial in progress of aurothiomalate: https://clinicaltrials.gov/ct2/show/NCT00575393.

(4) (a) Berners-Price, S. J.; Filipovska, A. Gold Compounds as Therapeutic Agents for Human Diseases. *Metallomics* **2011**, *3*, 863−873; (b) Bindoli, A.; Rigobello, M. P.; Scutari, G.; Gabbiani, C.; Casini, A.; Messori, L. Thioredoxin Reductase: A Target for Gold Compounds Acting as Potential Anticancer Drugs. *Coord. Chem. Rev.* **2009**, *253*, 1692−1707.

(5) (a) Ali, M.; Dondaine, L.; Adolle, A.; Sampaio, C.; Chotard, F.; Richard, P.; Denat, F.; Bettaieb, A.; Le Gendre, P.; Laurens, V.; Goze, C.; Paul, C.; Bodio, E. Anticancer Agents: Does a Phosphonium Behave Like a Gold(I) Phosphine Complex? Let a "Smart" Probe Answer!. *J. Med. Chem.* **2015**, *58*, 4521−4528. (b) Bazzicalupi, C.; Ferraroni, M.; Papi, F.; Massai, L.; Bertrand, B.; Messori, L.; Gratteri, P.; Casini, A. Determinants for Tight and Selective Binding of a Medicinal Dicarbene Gold(I) Complex to a Telomeric DNA G-Quadruplex: A Joint ESI MS and XRD Investigation. *Angew. Chem. Int. Ed.* **2016**, *55*, 4256–4259. (c) Laskay, A.; Garino, C.; Tsybin, Y. O.; Salassa, L.; Casini, A. Gold Finger Formation Studied by High-Resolution Mass Spectrometry and *In Silico* Methods. *Chem. Commun.* **2015**, *51*,1612-1615. (d). McKeage, M. J.; Maharaj, L.; Berners-Price, S. J. Mechanisms of Cytotoxicity and Antitumor Activity of Gold(I) Phosphine Complexes: The Possible Role of Mitochondria. *Coord. Chem. Rev.* **2002**, *232*, 127–135.

(6) Visbal, R.; Fernández-Moreira, V.; Marzo, I.; Laguna, A.; Gimeno, M. C. Cytotoxicity and Biodistribution Studies of Luminescent Au(I) and Ag(I) N-Heterocyclic Carbenes. Searching for New Biological Targets. *Dalton Trans.* **2016**, *45*, 15026–15033. (b) Citta, A.; Schuh, E.; Mohr, F.; Folda, A.; Massimino, M. L.; Bindoli, A.; Casini, A.; Rigobello, M. P. Fluorescent Silver(I) and Gold(I)–*N*-Heterocyclic Carbene Complexes with Cytotoxic Properties: Mechanistic Insights. *Metallomics* **2013**, *5*, 1006-1015. (c) Bertrand, B.; de Almeida, A.; Van der Burgt, E. P. M.; Picquet, M.; Citta, A.; Folda, A.; Rigobello, M. P.; Le Gendre, P.; Bodio, E.; Casini, A. New Gold(I) Organometallic Compounds with Biological Activity in Cancer Cells. *Eur. J. Inorg. Chem.* **2014**, 4532-4536. (d) Tasan, S.; Zava, O.; Bertrand, B.; Bernhard, C.; Goze, C.; Picquet, M.; Le Gendre, P.; Harvey, P.; Denat, F.; Casini, A.; Bodio, E. BODIPY–Phosphane as a Versatile Tool for Easy Access to New Metal-Based Theranostics. *Dalton Trans.* **2013**, *42*, 6102-6109. (e) Langdon-Jones, E. E.; Lloyd, D.; Hayes, A. J.; Wainwright, S. D.; Mottram, H. J.; Coles, S. J.; Horton, P. N.; Pope, S. J. A. Alkynyl-Naphthalimide Fluorophores: Gold Coordination Chemistry and Cellular Imaging Applications. *Inorg. Chem.* **2015**, *54*, 6606-6615. (f) Balasingham, R. G.; Williams, C. F.; Mottram, H. J., Coogan, M. P.; Pope, S. J. A. Gold(I) Complexes Derived from Alkynyloxy-Substituted Anthraquinones: Syntheses, Luminescence, Preliminary Cytotoxicity, and Cell Imaging Studies. *Organometallics* **2012**, *31*, 5835–5843.

(7) (a) Loudet, A.; Burgess, K. BODIPY Dyes and Their Derivatives: Syntheses and Spectroscopic Properties. *Chem. Rev.* **2007**, *107*, 4891-4932; b) Ulrich, G.; Ziessel, R.; Harriman, A. The Chemistry of Fluorescent Bodipy Dyes: Versatility Unsurpassed. *Angew. Chem., Int. Ed.* **2008**, *47*, 1184-1201.

(8) Terai, T.; Nagano, T. Small-Molecule Fluorophores and Fluorescent Probes for Bioimaging. *Pflugers Arch. – Eur. J. Physiol.* **2013**, *465*, 347-359.

(9) Boselli, L.; Carraz, M.; Mazères, S.; Paloque, L.; González, G.; Benoit-Vical, F.; Valentin, A.; Hemmert, C.; Gornitzka, H. Synthesis, Structures, and Biological Studies of Heterobimetallic Au(I)–Ru(II) Complexes Involving N-Heterocyclic Carbene-Based Multidentate Ligands. *Organometallics* **2015**, *34*, 1046–1055.

(10) Fernández-Moreira, V.; Marzo, I.; Gimeno, M. C. Luminescent Re(I) And Re(I)/Au(I) Complexes as Cooperative Partners in Cell Imaging and Cancer Therapy. *Chem. Sci*. **2014**, *5*, 4434-4446.

(11) (a) Fernández-Moreira, V.; Thorp-Greenwood, F. L.; Coogan, M. P. Application of d^6 Transition Metal Complexes in Fluorescence Cell Imaging. *Chem. Commun*. **2010**, *46*, 186-202. (b) Lo, K. K.-W.; Louie, M.-W.; Zhang, K. Y. Design of Luminescent Iridium(III) and Rhenium(I) Polypyridine Complexes as *in Vitro* and *in Vivo* Ion, Molecular and Biological Probes. *Coord. Chem. Rev.* **2010**, *254*, 2603-2622. (c) Zhao, Q.; Huang, C.; Li, F. Phosphorescent Heavy-Metal Complexes for Bioimaging. *Chem. Soc. Rev.* **2011**,*40*, 2508–2524; c) Thorp-Greenwood, F. L. An Introduction to Organometallic Complexes in Fluorescence Cell Imaging: Current Applications and Future Prospects. *Organometallics* **2012**, *31*, 5686-5692. (d) Coogan, M. P.; Fernández-Moreira, V. Progress with, and Prospects for, Metal Complexes in Cell Imaging. *Chem. Commun.* **2014**, *50*, 384-399; e) Lo, K. K.-W. Luminescent Rhenium(I) and Iridium(III) Polypyridine Complexes as Biological Probes, Imaging Reagents, and Photocytotoxic Agents. *Acc. Chem. Res.* **2015**, *48*, 2985-2995.

(12) Wenzel, M.; Bigaeva, E.; Richard, P.; Le Gendre, P.; Picquet, M.; Casini, A.; Bodio, New Heteronuclear Gold(I)–Platinum(II) Complexes with Cytotoxic Properties: Are Two Metals Better Than One? E. *J. Inorg. Biochem.* **2014**, *141*, 10–16.

(13) Bertrand, B.; Citta, A.; Franken, I. L.; Picquet, M.; Folda, A.; Scalcon, V.; Rigobello, M. P.; Le Gendre, P.; Casini, A.; Bodio, E. Gold(I) NHC-Based Homo- and Heterobimetallic Complexes: Synthesis, Characterization and Evaluation as Potential Anticancer Agents. *J. Biol. Inorg. Chem.* **2015**, *20*, 1005–1020.

(14) Montalbetti, C. A. G. N.; Falque, V. Amide Bond Formation and Peptide Coupling. *Tetrahedron* **2005**, *61*, 10827–10852.

(15) Gunatilleke, S. S.; Barrios, A. M. Tuning The Au(I)-Mediated Inhibition of Cathepsin B Through Ligand Substitutions. *J. Inorg. Biochem.* **2008**, *102*, 555–563.

(16) Fernández-Moreira, V.; Thorp-Greenwood, F. L.; Amoroso, A. J.; Cable, J.; Court, J. B.; Gray, V.; Hayes, A. J.; Jenkins, R. L.; Kariuki, B. M.; Lloyd, D.; Millet, C. O.; Williams, C. F.; Coogan, M. P. Uptake and Localisation of Rhenium *Fac*-Tricarbonyl Polypyridyls in Fluorescent Cell Imaging Experiments. *Org. Biomol. Chem.* **2010**, *8*, 3888–3901.

(17) Amoroso, A. J.; Arthur, R. J.; Coogan, M. P.; Court, J. B.; Fernández-Moreira, V.; Hayes, A. J.; Lloyd, D.; Millet, C.; Pope, S. J. A. 3-Chloromethylpyridyl Bipyridine *Fac*-Tricarbonyl Rhenium: A Thiol-Reactive Luminophore for Fluorescence Microscopy Accumulates in Mitochondria. *New J. Chem.* **2008**, *32*, 1097–1102.

(18) Dattelbaum, D. M.; Omberg, K. M.; Schoonover, J. R.; Martin, R. L.; Meyer, T. J. Application of Time-Resolved Infrared Spectroscopy to Electronic Structure in Metal-to-Ligand Charge-Transfer Excited States. *Inorg. Chem.* **2002**, *41*, 6071-6079.

(19) (a) Kirgan, R. A.; Sullivan, B. P.; Rillema, D. P. Photochemistry and Photophysics of Coordination Compounds: Rhenium. *Top Curr. Chem.* Eds.; Wiley, **2007**, *281*, 45-100. (b) Casula, A.; Nairi, V.; Fernández-Moreira, V.; Laguna, A.; Lippolis, V., Garau, A., Gimeno, M. C. Re(I) Derivatives Functionalised with Thioether Crowns Containing the 1,10-Phenanthroline Subunit as a New Class of Chemosensors. *Dalton Trans.* **2015**, *44*, 18506-18517. (c) Yam, V. W.-W; Cheng, E. C.-C. Photochemistry and Photophysics of Coordination Compounds: Gold. *Top Curr. Chem.* **2007**, *281*, 269–309.

(20) (a) Baiano, J. A.; Carlson, D. L.; Wolosh, G. M.; DeJesus, D. E.; Knowles, C. F.; Szabo Jr., E. G.:, Murphy, W. R. Bimetallic Complexes of Rhenium(1). Preparation of $Re(BL)(C0)_3Cl$ and $[Re(CO)_3Cl]_2(BL)$ (BL = 2,3-Bis(2-pyridyl)pyrazine, 2,3-Bis(2-pyridyl)quinoxaline, and 2,3-Bis(2-pyridyl) benzo[*g*]quinoxaline). *Inorg. Chem.* **1990**, *29*, 2321-2332. (b) Cleary, R. L.; Byrom, K. J.; Bardwell, D. A.; Jeffery, J. C.; Ward, M. D.; Calogero, G.; Armaroli, N.; Flamigni, L.; Barigelletti, F. Intercomponent Electronic Energy Transfer in Heteropolynuclear Complexes Containing Ruthenium- and Rhenium-Based Chromophores Bridged by an Asymmetric Quaterpyridine Ligand. *Inorg. Chem.*, **1997**, *36*, 2601–2609.

(21) Fernández-Moreira, V.; Ortego, M. L.; Williams, C. F.; Coogan, M. P.; Villacampa, M. D.; Gimeno, M. C. Bioconjugated Rhenium(I) Complexes with Amino Acid Derivatives: Synthesis, Photophysical Properties, and Cell Imaging Studies. *Organometallics* **2012**, *31*, 5950-5957 (b) Kuimova, M. K.; Alsindi, W. Z.; Blake, A. J.; Davies, E. S.; Lampus, D. J.; Matousek, P.;

McMaster, J.; Parker, A. W.; Towrie, M.; Sun, X.-Z.; Wilson, C.; George, M. W. Probing the Solvent Dependent Photophysics of *fac*-[Re(CO)$_3$(dppz-X$_2$)Cl] (dppz-X$_2$ = 11,12-X$_2$ dipyrido[3,2-a:2′,3′-c]phenazine); X = CH$_3$, H, F, Cl, CF$_3$). *Inorg. Chem.* **2008**, *47*, 9857-9869.

(22) Thorp-Greenwood, F. L.; Platts, J. A.; Coogan, M. P. Experimental and Theoretical Characterisation of Phosphorescence from Rhenium Polypyridyl Tricarbonyl Complexes. *Polyhedron* **2014**, *67*, 505–512. (b) Kumar, A.; Sun, S.-S.; Lees, A.-L. Photophysics and Photochemistry of Organometallic Rhenium Diimine Complexes. *Top. Organomet. Chem.* **2010**, *29*, 1-35.

(23) Sacksteder, L. A.; Lee, M.; Demas, J. N.; DeGraff, B. A. Long-Lived, Highly Luminescent Rhenium(I) Complexes as Molecular Probes: Intra- and Intermolecular Excited-State Interactions. *J. Am. Chem. Soc.* **1993**, *115*, 8230-8232.

(24) (a) Wallace, L.; Rillema, D. P. Photophysical Properties Of Rhenium(I) Tricarbonyl Complexes Containing Alkyl- And Aryl-Substituted Phenanthrolines As Ligands. *Inorg. Chem.* **1993**, *32*, 3836-3843; (b) Bertrand, H. C.; Clède, S.; Guillot, R.; Lambert, F.; Policar, C. Luminescence Modulations of Rhenium Tricarbonyl Complexes Induced by Structural Variations. *Inorg. Chem.* **2014**, *53*, 6204−6223; (c) Wenger, O. S.; Henling, L. M.; Day, M. W.; Winkler, J. R.; Gray, H. B. Photoswitchable Luminescence of Rhenium(I) Tricarbonyl Diimines. *Inorg. Chem.* **2004**, *43*, 2043–2048.

(25) Gutiérrez, A.; Gracia-Fleta, L.; Marzo, I.; Cativiela, C.; Laguna, A.; Gimeno, M. C. Gold(I) Thiolates Containing Amino Acid Moieties. Cytotoxicity and Structure–Activity Relationship Studies. *Dalton Trans.* **2014**, *43*, 17054-17066.

(26) Fernández-Moreira, V.; Sastre-Martín, H. Photophysical and Bioactivity Behavior of Fac-Rhenium(I) Derivatives Containing Ditopic Sulfurpyridine Ligands. *Inorg. Chim. Acta* **2017**, *46*, 127–133.

(27) Wenzel, M.; Bertrand, B.; Eymin, M.-J.; Comte, V.; Harvey, J. A.; Richard, P.; Groessl, M.; Zava, O.; Amrouche, H.; Harvey, P. D.; Le Gendre, P.; Picquet, M.; Casini, A. Multinuclear Cytotoxic Metallodrugs: Physicochemical Characterization and Biological Properties of Novel Heteronuclear Gold–Titanium Complexes. *Inorg. Chem.* **2011**, *50*, 9472–9480.

(28) Frik, M.; Fernández-Gallardo, J.; Gonzalo, O.; Mangas-Sanjuan, V.; González-Álvarez, M.; Serrano del Valle, A.; Hu, C.; González-Álvarez, I.; Bermejo, M.; Marzo I.; Contel, M. Cyclometalated Iminophosphorane Gold(III) and Platinum(II) Complexes. A Highly Permeable Cationic Platinum(II) Compound with Promising Anticancer Properties. *J. Med. Chem.* **2015**, *58*, 5825-5841.

(29) Ye, R.-R.; Tan, C.-P.; Lin, Y.-N.; Ji, L.-N.; Mao, Z.-W. A Phosphorescent Rhenium(I) Histone Deacetylase Inhibitor: Mitochondrial Targeting and Paraptosis Induction. *Chem. Commun.* **2015**, *51*, 8353-8356. (b) Louie, M.-W.; Liu, H.-W.; Lam, M. H.-C.; Lam, Y.-W.; Lo, K. K.-W. Luminescent Rhenium(I) Polypyridine Complexes Appended with an α-D-Glucose Moiety as Novel Biomolecular and Cellular Probes. *Chem. - Eur. J.* **2011**, *17*, 8304−8308.

(30) Mármol, I.; Virumbrales-Muñoz, M.; Quero, J.; Sánchez-de-Diego, C.; Fernández, L.; Ochoa, I.; Cerrada, E.; Yoldi, M. J. R. Alkynyl gold(I) complex triggers necroptosis via ROS generation in colorectal carcinoma cells. *J. Inorg. Biochem.* **2017**, *176*, 123–133.

(31) Barnard, P. J.; Berners-Price, S. J. Targeting the Mitochondrial Cell Death Pathway with Gold Compounds. *Coord. Chem. Rev.* **2007**, *251*, 1889-1902.

(32) Clède, S.; Lambert, F.; Saint-Fort, R.; Plamont, M.-A., Bertrand, H. ; Vessières, A.; Policar, C. Influence of the Side-Chain Length on the Cellular Uptake and the Cytotoxicity of Rhenium Triscarbonyl Derivatives: A Bimodal Infrared and Luminescence Quantitative Study. *Chem. Eur. J.* **2014**, *20*, 8714–8722.

(33) Coogan, M. P.; Fernández-Moreira, V.; Hess, J. B.; Pope, S. J. A.; Williams, C. Rhenium Fac-Tricarbonyl Bisimine Complexes: Luminescence Modulation by Hydrophobically Driven Intramolecular Interactions. *New J. Chem.* **2009**, *33*, 1094–1099.

(34) Sirajuddin, M.; Ali, S.; Badshah, A. Drug-DNA Interactions and their Study By Uv-Visible, Fluorescence Spectroscopies and Cyclic Voltametry. *J. Photochem. Photobiol. B. Biol.* **2013**, *124*, 1-19.

(35) Krishnamoorthy, P.; Sathyadevi, P.; Cowley, A. H.; Butorac, R. R.; Dharmaraj, N. Evaluation of DNA Binding, DNA Cleavage, Protein Binding and *in Vitro* Cytotoxic Activities of Bivalent Transition Metal Hydrazone Complexes. *Eur. J. Med. Chem.* **2011**, *46*, 3376-3387.

(36) Reichmann, M. E.; Rice, S. A.; Thomas, C. A.; Doty, P. A. Further Examination of the Molecular Weight and Size of Desoxypentose Nucleic Acid. *J. Am. Chem. Soc*. **1954**, *76*, 3047-3053.

(37) Wolfe, A.; Shimer, G. H.; Meehan, T. Polycyclic Aromatic Hydrocarbons Physically Intercalate Into Duplex Regions of Denatured DNA. *Biochemistry* **1987**, *26*, 6392-6396.

(38) Usón, R.; Laguna, A.; Laguna, M. (Tetrahydrothiophene)Gold(I) or Gold(III) Complexes. *Inorg. Synth.* **1989**, *26*, 85–91.

(39) Wang, Y.; Lucia, L. A.; Schanze, K. S. C-C Bond Fragmentation as a Probe for Photoinduced Intramolecular Electron Transfer *J. Phys. Chem.* **1995**, *99*, 1961-1968.

(40) (a) Doulain, P.-E.; Decréau, R.; Racoeur, C.; Goncalves, V.; Dubrez, L.; Bettaieb, A.; Le Gendre, P.; Denat, F.; Paul, C.; Goze, C.; Bodio E. Towards the elaboration of new gold-based optical theranostics. *Dalton Trans.*, **2015**, *44*, 4874–4883; (b) Montanel-Pérez, S.; *Síntesis de carbenos acíclicos de oro. Funcionalización de metalaciclos. Estudio de sus propiedades biológicas.* **2014**, 237-240.

For Table of Contents

Trackable metallodrugs combining luminescent Re(I) and bioactive Au(I) fragments

Andrés Luengo, Vanesa Fernández-Moreira,* Isabel Marzo and M. Concepción Gimeno*

Trackable metallodrugs were throughly developed by the combination of both, a luminescent Re(I) and a bioactive Au(I) metallofragment connected by a suitable ditopic ligands.